A PARASITIC LOAD SPEED CONTROL FOR DYNAMIC SPACE POWER SYSTEMS

A Thesis

Presented to

the Faculty of the School of Engineering and Applied Sciences

University of Virginia

In Partial Fulfillment

of the Requirements for the Degree

Master of Electrical Engineering

by

Hugh Milton Holt

August 1969

ACKNOWLEDGEMENT

This work was accomplished through the helpful guidance of my advisor, Mr. Mark G. Foster of the University of Virginia, and through the generous cooperation of Mr. Robert C. Wells and others of NASA Langley Research Center. The author greatly appreciates this assistance.

ABSTRACT

A method for controlling the speed of a dynamic space power system by a parasitic electric load technique is investigated. A mathematical representation of the power system and speed control is developed. From this model, a linear approximation is utilized to synthesize a compensation network that will produce a specified response in the rotational speed of the power system to a change in electrical load. It is shown that the compensation network can be modified to accommodate a wide range of responses for dynamic power systems. Curves are given that display the response of a model of the control changes in operational load. The model of the control includes the compensation network and analog simulations of a frequency sensor, a parasitic load, and the rotating unit. Finally, problems that are expected in the design of a parasitic load and in the integration of the control with the space power system are discussed.

APPROVAL SHEET

This thesis is submitted in partial fulfillment of

the requirements for the degree of

Master of Electrical Engineering

Author

Approved:

Faculty Adviser

Dean, School of Engineering
and Applied Science

August 1969

TABLE OF CONTENTS

LIST OF FIGURES

FIGURE PAGE

LIST OF TABLES

LIST OF SYMBOLS

A	gain of preamplifier
A1,A2,A3,A4,A5	amplifier
i,n	zero or positive integer
CRU	combined rotating unit
C_1, C_2, C_f	capacitor
C(s)	control variable
$E_p(s)$	load error
$E_r(s)$	input error
F(s)	frequency of alternator in Laplace domain
F_o	magnitude of reference frequency
$F_r(s)$	reference frequency in Laplace domain
f(t)	frequency of the alternator in time domain
$f_r(t)$	reference frequency in time domain
$G_a(s)$	transfer function of the alternator
$G_e(s)$	transfer function of the compensation network
I	integrating amplifier
J	moment of inertia
K_c	gain of the compensation network
K_i	inertia constant of rotating unit
K_p	magnitude of operational load
K, K_T	constant
P_d	difference between input and output power

P_e	electromagnetic power
P_l	operational load
P_p	parasitic load
P_{sh}	mechanical shaft power
p	number of poles on the alternator
P_i	poles of the compensation network
R_{1-6}, R_i, R_f, R_s	resistor
R(s)	reference variable
s	Laplace operator
T	temperature
$T_e(t)$	electromagnetic torque
$T_i(t)$	inertia torque
$T_{sh}(t)$	mechanical shaft torque
u(s)	unit step function
V	supply voltage
V_a	output voltage of preamplifier
V_e	voltage proportional to frequency error
V_i	input voltage to the compensation amplifier
V_p	voltage proportional to parasitic load
Z_f, Z_2	feedback impedance
Z_i, Z_1	input impedance
Z_o	zero of the transfer function for the compensation network
Z_i	zeros of the compensation network

α	accuracy of control
δ, θ	angle in radians
$\delta(s)$	unit impulse function
ζ	damping ratio
$\omega(t)$	angular velocity
ω_n	undamped natural frequency
ω_o	initial frequency

CHAPTER I

INTRODUCTION

For long-term space explorations electrical power systems that utilize regenerative processes rather than expendable-mass or storage techniques are needed. Dynamic power systems based on closed-loop thermodynamic cycles, such as the Rankine liquid-gas and Brayton gas cycles, appear as potentially feasible systems. However, for space applications these systems, which convert heat energy into electrical energy by a turboalternator located in the working-fluid loop, have one important disadvantage. Because certain spacecraft loads operate only within a narrow range of frequencies, the speed of the compressor-turbine-alternator rotating unit must be carefully controlled.

Since constant speed of the combined rotating unit (CRU) can be obtained only if input power to the turbine always equals output power, speed control must involve either adjusting input power to equal output power or vice versa. Although there are several conceivable means of achieving this balance, few methods are acceptable from a practical engineering viewpoint.

Input power can be regulated by varying the heat content of the working fluid or by adjusting the flow of the heated fluid through the turbine. A control based on changing the heat energy of the working

fluid would involve equipment for adjusting the heat energy delivered by the source or for jettisonning excess heat to space. For example, in a system where the heat source is a nuclear reactor, rods for controlling the nuclear reaction or a system of louvers for rejecting excess heat might be used for control. Because this type of hardware would, in general, contribute significantly to the complexity of the dynamic power systems presently being designed and might introduce problems in integrating the power system with the rest of the spacecraft, such a control has received little consideration.

A control that functions by adjusting the flow of heated fluid through the turbine has been shown feasible. In a study by Thomas[1] valves were used for bypassing portions of the fluid around the turbine. Although this type of control is attractive for short missions, for long-term missions changes in the flow characteristics of the valves, which would adversely affect the performance of the control, are to be expected. In addition, because of the location of the valves in the working-fluid loop, corrective maintenance in the case of breakdown during manned missions would be difficult.

Output power can be controlled by modulating the electrical load connected to the alternator. This can be done by varying the operational load of the spacecraft or by using a parasitic load on the alternator. A control based on maintaining the operational load of

---

[1]Ronald L. Thomas, "Turboalternator Speed Control with Valves in Two-Spool Solar Brayton System," National Aeronautics and Space Administration TN D-3783 (January, 1967).

the spacecraft at a level that always balances the input to the turbine would require a precise knowledge of the size and duty cycle of each load. A load-handling system would be needed for scanning all available loads and for switching on or off loads as needed for restoring equilibrium. Since most loads do not have a constant duty cycle and since a system for sequencing of loads would be complex, this method of control is impractical.

A parasitic load on the alternator can be used in two ways for speed control. First, each operational load can be duplicated by a parasitic load. When an operational load is removed from the alternator, the corresponding parasitic load is added and vice versa. It is not, however, a simple matter to duplicate operational loads because, as was said before, most loads do not have a constant duty cycle. In addition, this approach involves an uneconomical use of power because no sequencing of loads can be used. The average demand on the power system will be greatly increased with a corresponding increase in the size and weight of the system.

A second way of using a parasitic load for speed control involves a variable parasitic load that is added to or removed from the alternator as a function of the unbalance between the input and output of the turbine. This type of control has several advantages for space applications. The power profile for each individual load does not have to be known. The change in CRU speed can be used directly or indirectly as the control variable, which eliminates complex scanning systems. Since the control can be designed using solid-state

components, the size and weight of the control make for easy incorporation into presently available power systems. The control involves no moving parts. Because access to the working-fluid loop is not required, the control can be located remotely from the power system.

Few studies of parasitic load speed controls for space power systems have been reported. Dauterman[2] and Lalli[3] have designed controls for power systems based on the Rankine liquid-gas cycle. Personnel of Lewis Research Center[4,5] have described controls for Brayton-cycle power systems. Because these controls for the most part have been developed around arbitrary design specifications, there exists a need for an analytical study of parasitic load speed controls.

It is the purpose of this thesis to develop an analytical model for a variable parasitic load speed control and to show through the use of the digital computer how this model can be used for designing a speed control that responds in a given manner. To establish the

---

[2]W. E. Dauterman, "Snap 2 Power Conversion System Topical Report No. 18," Thompson Ramo Wooldridge Inc. Report No. ER-5075 (December, 1963).

[3]V. R. Lalli, "Sunflower Rotational Speed Control Topical Report," Thompson Ramo Wooldridge Inc. Report No. ER-4947 (March, 1963).

[4]John L. Word and others, "Static Parasitic Speed Controller for Brayton-Cycle Turboalternator," National Aeronautics and Space Administration TN D-2176 (September, 1967).

[5]Roy C. Tew and others, "Analog-Computer Study of Parasitic-Load Speed Control for Solar-Brayton System Turboalternator," National Aeronautics and Space Administration TN D-3784 (January, 1967).

validity of the model, a control is designed for a specific Brayton-cycle space power system. The response of the control is verified through use of analog computer simulations in conjunction with "bread-board" hardware.

CHAPTER II

ANALYTICAL DEVELOPMENT OF A PARASITIC LOAD SPEED CONTROL

In the development of a parasitic-load speed control, an analysis of the dynamics of the CRU must first be made. For the system diagrammed in Figure 1, the operation of the alternator can be expressed in terms of three classes of torque acting on the rotating members: an inertia torque, $T_i(t)$; an electromagnetic torque, $T_e(t)$; and a mechanical shaft torque, $T_{sh}(t)$, representing input from the turbine. The relationship is:

$$T_i(t) + T_e(t) = T_{sh}(t) \tag{1}$$

The inertia torque, as is shown in Appendix I, can be written

$$T_i(t) = J \frac{d\omega(t)}{dt}$$

where J is the moment of inertia and ω is the angular velocity. The electromagnetic torque is given by

$$T_e(t) = \frac{P_e(t)}{\omega(t)}$$

where $P_e(t)$ is the electromagnetic power, which represents the electrical load on the alternator. Similarly,

$$T_{sh}(t) = \frac{P_{sh}(t)}{\omega(t)}$$

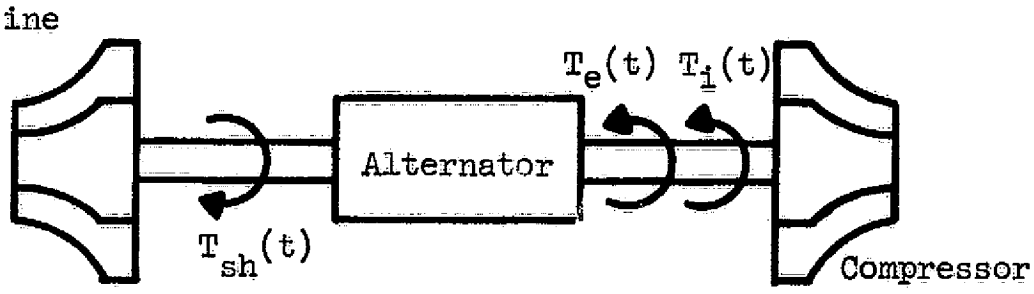

Figure 1.- Torques present in the compressor-turbine-alternator rotating unit

where $P_{sh}(t)$ is the mechanical shaft power. Substituting these expressions into equation (1) gives

$$J \frac{d\omega(t)}{dt} + \frac{P_e(t)}{\omega(t)} = \frac{P_{sh}(t)}{\omega(t)} \tag{2}$$

On rearranging and integrating, equation (2) becomes

$$\omega(t) = \left\{ \frac{2}{J} \int \left[P_{sh}(t) - P_e(t) \right] dt + \omega_o^2 \right\}^{1/2} \tag{3}$$

Change in the angular velocity of the CRU will be properly limited if the integral term of equation (3) is kept small. Speed control can, therefore, be achieved by insuring that the difference between $P_{sh}(t)$ and $P_e(t)$ always approaches zero. A convenient way of obtaining this condition is to vary $P_e(t)$ by using a parasitic electrical load in conjunction with operational loads of the spacecraft.

Because parasitic load cannot be added or removed instantaneously when the operational load varies, some change in the speed of the CRU is inevitable. Since the size of the change reflects the response time of the control system for the parasitic load, the method by which a difference between $P_{sh}(t)$ and $P_e(t)$ is detected becomes a critical aspect of the control system.

The control could operate by sensing the total electrical power connected to the alternator. However, devices for producing an analog signal proportional to average power, such as thermal converters and Hall effect converters, have inherently slow response times. Moreover, since the waveform of the alternator may be distorted as a

consequence of the conversion of a large amount of power to dc, Hall effect devices, being sensitive to waveform, are unsuitable.

The control could operate by sensing the rotational speed of the alternator. A wide selection of speed sensing devices, such as dc generators, inductance probes, and magnetic probes, is available. These devices have reasonable response times and operate independently of alternator waveform. But the use of such a control would require access to the CRU shaft, which presents two problems. In the first place, some part or all of the control would have to be mounted on the shaft. This would necessitate increasing the length of the shaft to accommodate the components and devising means of securing the components without adversely affecting the performance of the shaft. Secondly, the components mounted on the shaft would be subjected to rotational speeds as high as 64,000 revolutions per minute.[6] To find components that would operate satisfactorily for long periods of time under these conditions would be difficult.

Since the frequency of the alternator is directly related to the speed of the CRU by the number of poles on the alternator, the control could operate by sensing alternator frequency. This type of control is attractive for several reasons. Since the purpose of the parasitic load is to control the speed of the CRU, the control signal would be highly responsive to the controlled variable. Devices based on tuned

---

[6]G. G. McKhann, "Preliminary Design of Pu-237 Isotope Brayton-Cycle Power System for MORL" (Santa Monica, California), I, 4-73.

circuit or counting techniques for sensing frequency with a minimum of time delay are readily available. These devices also operate independently of alternator waveform. In addition, this type of control is adaptable to the design of the CRU since it can be connected directly to the alternator output terminals.

Thus, a plausible method for maintaining the speed of the CRU within a narrow range would consist of a variable parasitic electrical load with a control system for sensing alternator frequency. If the load of the spacecraft is decreased or switched off, the speed of the alternator and hence the frequency will increase. The control will detect this change in frequency and will react by gating current into the parasitic load to balance the load and turbine torques. Consequently, the average acceleration of the alternator will be reduced to zero. For an increase in vehicular load, the control will react to a decrease in alternator frequency by decreasing current into the parasitic load. The load and turbine torques will thus be balanced, and the acceleration of the alternator will be arrested.

For a control that operates by sensing frequency, the torque equation in terms of angular velocity can be expressed in terms of alternator frequency, f(t). This conversion is shown in Appendix I with the following results:

$$f(t) = \frac{p}{4\pi J} \int \left[\bar{T}_{sh}(t) - \bar{T}_e(t) \right] dt + \bar{F}_o \qquad (4)$$

where p is the number of poles on the alternator and F_o is the design frequency.

In order to control the frequency by manipulation of alternator load, equation (4) must be rewritten in terms of input and output power. This is done in Appendix II. The equation becomes

$$\frac{21.7\pi^2 J}{p^2} f(t) \frac{df(t)}{dt} = P_{sh}(t) - P_e(t) \qquad (5)$$

This equation is nonlinear due to the term on the left side. From a practical engineering viewpoint, two observations can be used for simplifying this equation. In the first place, since the purpose of the control is to control the speed of the CRU within a narrow range, the variations of the frequency, f(t), about the design frequency, F_o, must necessarily be small. Thus, an approximation to equation (5) can be made by substituting F_o for f(t). The equation now becomes linear.

$$\frac{21.7\pi^2 J}{p^2} F_o \frac{df(t)}{dt} = P_{sh}(t) - P_e(t) \qquad (6)$$

To show that equation (6) is a close approximation to equation (5), both equations can be solved for frequency as a function of time for a step change in $P_{sh}(t) - P_e(t)$. The solution for equation (5) is

$$f(t) = \left(2KP_d t + F_o^2\right)^{1/2}$$

where

$$K = \frac{p^2}{21.7\pi^2 J}$$

and F_d is the magnitude of the difference between $P_{sh}(t)$ and $P_e(t)$. The solution for equation (6) is

$$f(t) = \frac{KP_d}{F_o} t + F_o$$

By comparing the solutions for these two equations, as is done in Figure 2, one sees that for frequencies of $\pm$10 per cent of the design frequency the percentage of error introduced by the use of equation (6) rather than equation (5) does not exceed 0.7 per cent.

The second observation involves $P_{sh}(t)$. The power delivered to the turbine shaft is given by

$$P_{sh}(t) = \frac{5.4\pi}{p} T_{sh}(t)\, f(t)$$

This power as a function of frequency for a typical dynamic power system is plotted in Figure 3. It can be seen from this curve that for the proper choice of design speed the power delivered to the turbine shaft will be nearly constant for small variations of f(t) about the design frequency. For this analysis, therefore, P_{sh} can be assumed to be constant.

The change in output frequency as a function of input and output power can now be written

$$\frac{df(t)}{dt} = K_i \left\{ P_{sh} - \left[P_l(t) + P_p(t) \right] \right\} \qquad (7)$$

where

$$K_i = \frac{p^2}{21.7\pi J F_o}$$

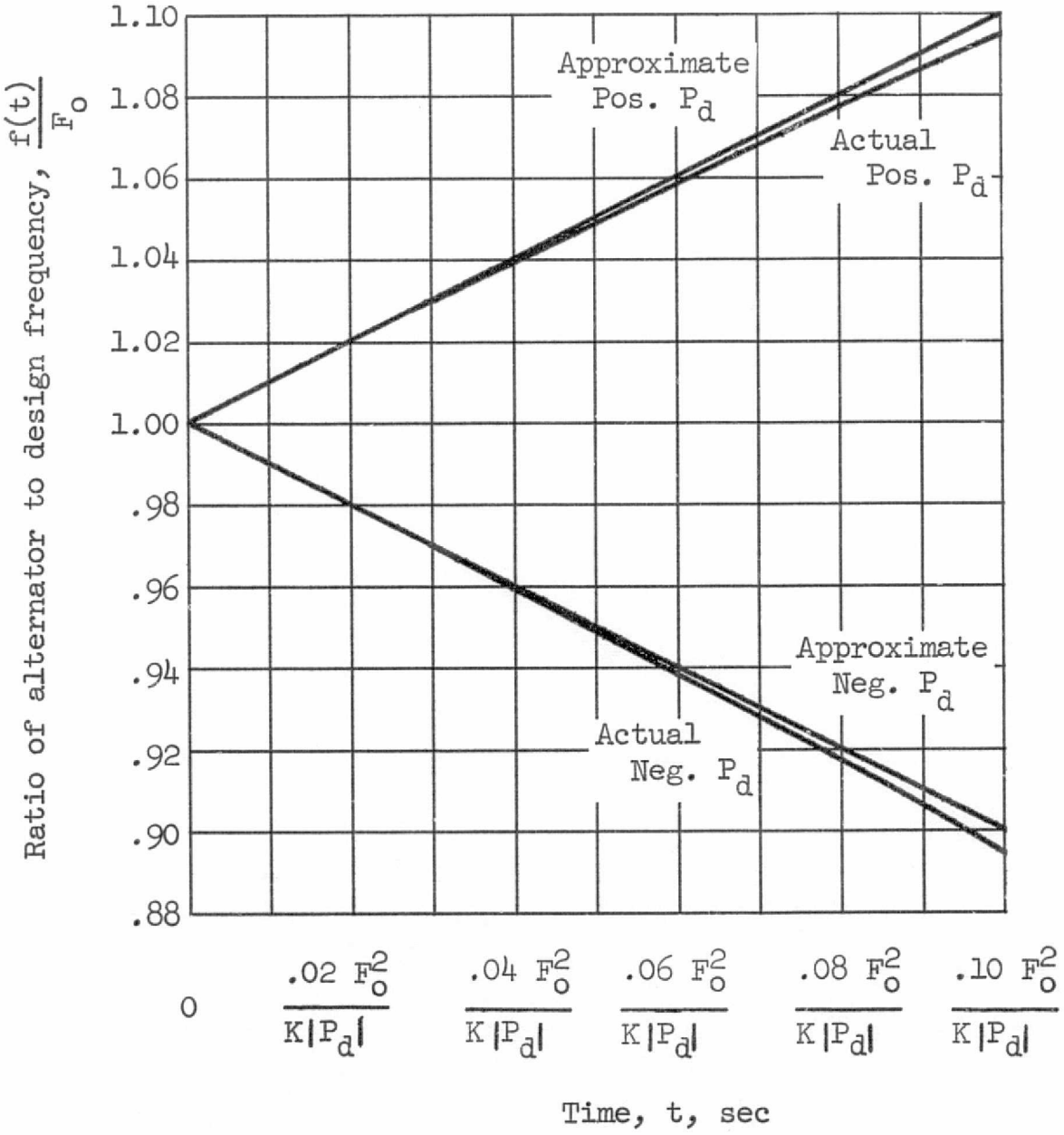

Figure 2.- Actual and linear approximation of alternator frequency for difference in input and output power of $\pm P_d$

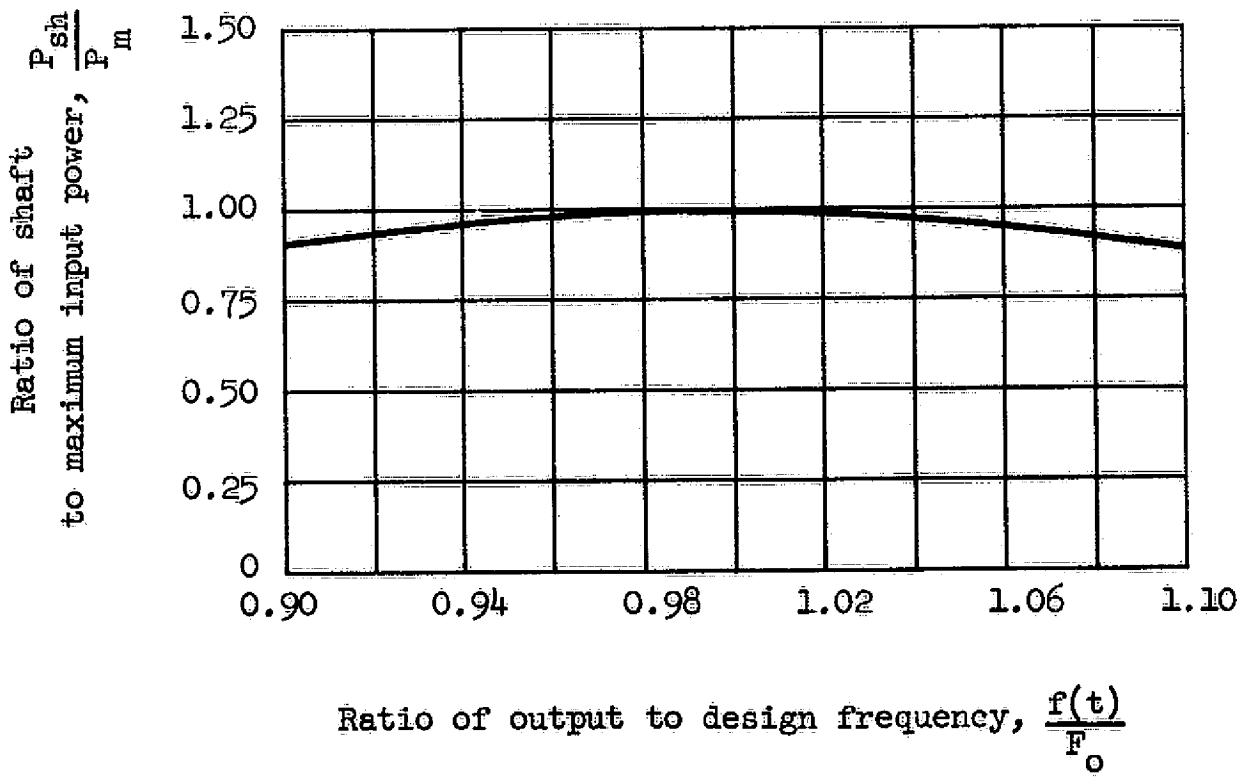

Figure 3.- Power delivered to the CRU shaft as a function of alternator frequency

and $P_e(t)$ is replaced by the sum of $P_l(t)$, the operational load, and $P_p(t)$, the parasitic load.

It can be seen from this equation that the frequency will increase at a constant rate for a decrease in operational load without a corresponding increase in parasitic load. It is also apparent that for an increase in operational load the frequency will decrease at a constant rate until a corresponding amount of parasitic load is removed or the CRU stalls. Thus, for the rotating unit to operate at the design frequency, the control must react to a change in alternator frequency by combining parasitic load with operational load until the combination exactly equals the input power to the shaft.

A system that can give the necessary control is one that can vary the parasitic load as a function of the error between a reference frequency and the actual alternator frequency. One such system is shown in the block diagram of Figure 4. In this figure $G_a(s)$ is the transfer function of the alternator and $G_c(s)$ is some compensation network. This network, using the error signal from the frequency sensor as an input, must produce an output proportional to the amount of parasitic load needed to restore the output frequency to its design value.

The transfer function for the alternator can be found from equation (7) and is given by

$$\frac{F(s)}{P_{sh}(s) - \left[P_l(s) + P_p(s)\right]} = \frac{K_i}{s}$$

where s is the Laplace operator.

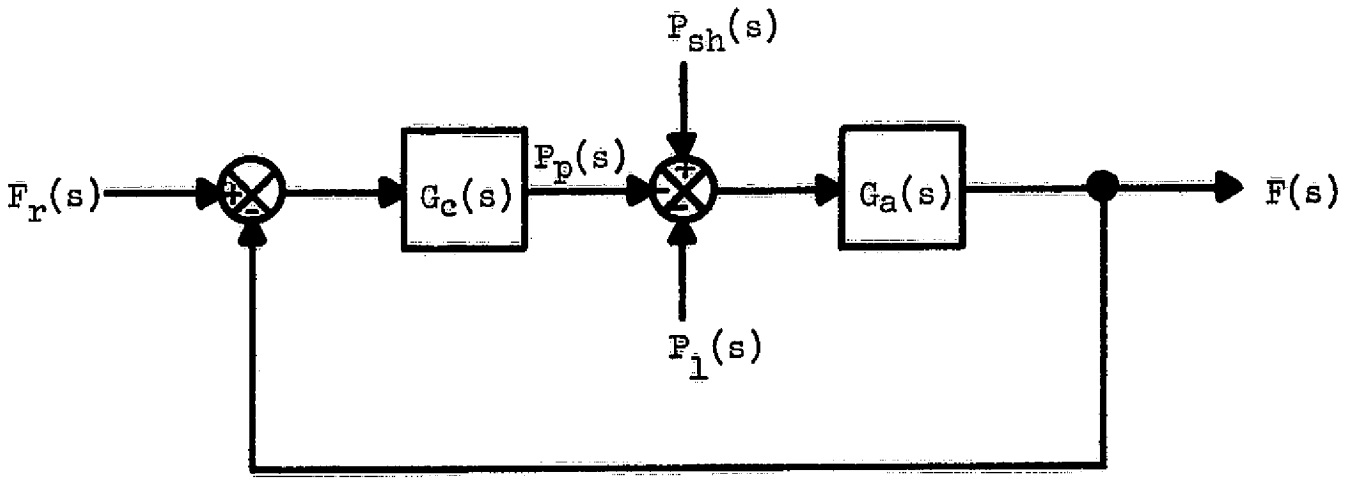

Figure 4.- Block Diagram for speed control system

The problem now is to determine $G_c(s)$ so that $f(t)$ is held equal to reference frequency, F_o, for a fixed shaft power and operational load and so that any deviation in $f(t)$ due to changes in operational load, $P_l(s)$, is held to a minimum.

By assuming $P_l(s)$ and $P_{sh}(s)$ as disturbance inputs in the block diagram, the response of the system for a reference input can be found. Thus,

$$\frac{F(s)}{F_r(s)} = \frac{- G_a(s)G_c(s)}{1 - G_a(s)G_c(s)}$$

For a unit step input the transfer function for $G_c(s)$ that will give a final value of $f(t)$ equal to the input can be synthesized. With a unit step input $F_r(s)$ equal to $\frac{F_o}{s}$, the final value theorem is used.

$$\lim_{t \to \infty} f(t) = \lim_{s \to 0} s\,F(s)$$

$$F(s) = \frac{- \frac{K_i}{s} G_c(s) \frac{F_o}{s}}{1 - \frac{K_i}{s} G_c(s)}$$

$$= \frac{K_i F_o G_c(s)}{s\left[s - K_i G_c(s)\right]}$$

The final value for $f(t)$ should approach F_o.

$$\lim_{s \to 0} sF(s) = F_o$$

$$= \lim_{s \to 0} \frac{- sK_i F_o G_c(s)}{s\left[s - K_i G_c(s)\right]}$$

By rearranging

$$F_o = \lim_{s \to 0} \frac{F_o}{1 - \frac{s}{K_i G_c(s)}}$$

In order for the right side of the equation to equal F_o,

$$\lim_{s \to 0} - \frac{s}{K_i G_c(s)} \to 0$$

An amplifier with a gain of K_c or a network with a transfer function of the form

$$G_c(s) = - K_c \frac{(s + Z_o)(s + Z_1) \cdots (s + Z_i) \cdots (s + Z_n)}{(s + P_o)(s + P_1) \cdots (s + P_i) \cdots (s + P_n)} \qquad (8)$$

will satisfy this equation. Since the rate at which F(s) approaches F_o is determined by $G_c(s)$, the transfer function should become as large as possible as s approaches zero.

The final value theorem can be used again to determine the steady state response for f(t) with a disturbance input $P_1(s)$. The transfer function for the system with a disturbance is

$$\frac{F(s)}{P_1(s)} = \frac{- G_a(s)}{1 - G_a(s) G_c(s)}$$

For a step input $P_1(s) = \frac{K_p}{s}$

$$F(s) = \frac{\frac{- K_i K_p}{s^2}}{1 - \frac{K_i G_c(s)}{s}}$$

$$= \frac{- K_i K_p}{s \left[s - K_i G_c(s) \right]}$$

Since the final value for f(t) should approach zero, the final value theorem gives

$$\lim_{s \to 0} s\, F(s) = \lim_{s \to 0} \frac{-K_i K_p}{s - K_i G_c(s)}$$

$$\lim_{s \to 0} s\, F(s) \to 0$$

This equation can be satisfied only if

$$\lim_{s \to 0} -K_i G_c(s) \to \infty$$

A $G_c(s)$ with a gain that approaches infinity or one with the form

$$G_c(s) = -K_c \frac{(s + Z_o)(s + Z_1) \cdots (s + Z_i) \cdots (s + Z_n)}{(s + P_o)(s + P_1) \cdots (s + P_i) \cdots (s + P_n)}$$

where the numerator becomes very much larger than the denominator as s approaches zero will satisfy this condition.

A comparison of this $G_c(s)$ with that of equation (8) shows them to be identical. The simplest form of the transfer function would be for $G_c(s)$ equal $-K_c$. In order that f(t) approach zero for disturbance inputs, K_c must then approach infinity. Now, in the actual speed control this transfer function will be approximated by an amplifier. If this particular function is used, problems associated with stability and control of amplifiers with high gains are to be expected. This difficulty can be avoided by using a compensation network of the form

$$G_c(s) = -K_c \frac{s + Z_o}{s} \tag{9}$$

This function does not require the use of a high gain amplifier but does satisfy all conditions for $G_c(s)$.

With this $G_c(s)$, the transfer function for the system with a reference input is

$$\frac{F(s)}{F_r(s)} = \frac{K_i K_c (s + Z_o)}{s^2 + K_i K_c s + K_i K_c Z_o}$$

and for the system with a disturbance input is

$$\frac{F(s)}{P_l(s)} = \frac{- K_i s}{s^2 + K_i K_c s + K_i K_c Z_o}$$

The latter transfer function can be written in terms of the natural frequency of oscillation and the damping ratio as follows:

$$\frac{F(s)}{P_l(s)} = \frac{- K_i s}{s^2 + 2\zeta\omega_n s + \omega_n^2} \tag{10}$$

where

$$\zeta = 1/2 \left(\frac{K_i K_c}{Z_o} \right)^{1/2} \tag{11}$$

$$\omega_n = (K_i K_c Z_o)^{1/2} \tag{12}$$

Since the primary concern in system operation is the response due to load changes, equation (10) can be used to determine values for K_c and Z_o that will give acceptable deviations in the alternator frequency due to step changes in alternator load. With the step load $P_l(s) = - \frac{K_p}{s}$, this equation can be written

$$F(s) = \frac{K_i K_p}{s^2 + 2\zeta\omega_n s + \omega_n^2}$$

The solution as a function of time is found in Appendix III and for the general case has the form

$$f(t) = \left[\frac{K_p K_i}{\omega_n(\zeta^2-1)^{1/2}}\right] e^{-\zeta\omega_n t} \sinh\left[\omega_n(\zeta^2-1)^{1/2} t\right] \qquad (13)$$

This equation gives the frequency as a function of time for a compensation network that has a transfer function as shown in equation (9). Before this equation can be evaluated, values for ζ and ω_n must be known. Approximations to the actual curves can be drawn by comparing the transfer function for this system to similar transfer functions found in the literature. For example, Truxal[7] has plotted the impulse response for the transfer function

$$\frac{C(s)}{R(s)} = \frac{\omega_n^2}{s^2 + 2\zeta\omega_n s + \omega_n^2}$$

as shown in Figure 5. For the unit impulse $\delta(s) = 1$, the output $C(s)$ will become

$$C(s) = \frac{\omega_n^2}{s^2 + 2\zeta\omega_n s + \omega_n^2} \qquad (14)$$

Now the transfer function for the frequency control under study is

$$\frac{F(s)}{P_1(s)} = - \frac{K_i s}{s^2 + 2\zeta\omega_n s + \omega_n^2}$$

and for removal of a unit step load, $P_1(s) = - u(s) = - 1/s$, the output frequency will be

---

[7] John G. Truxal, Automatic Feedback Control System Synthesis (New York, 1968), p.39.

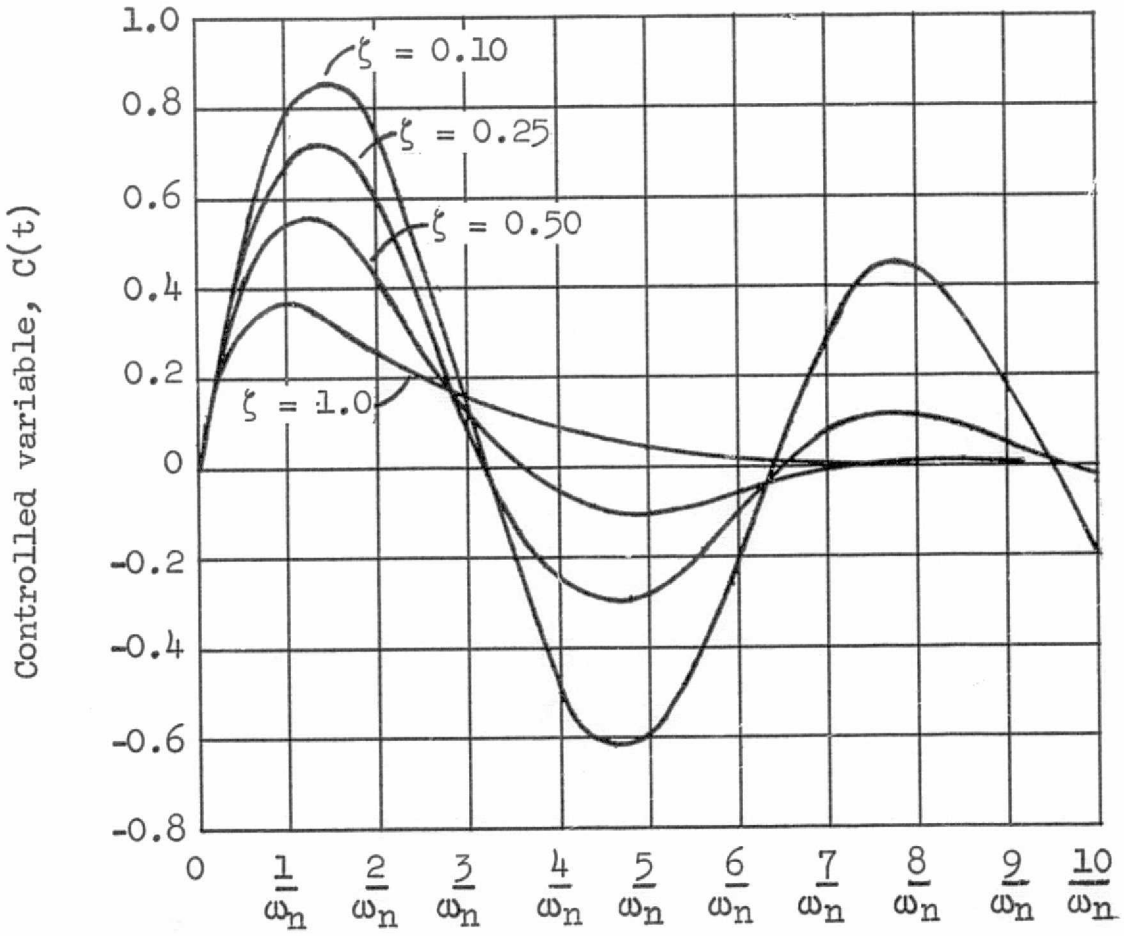

Figure 5.- Impulse response for transfer function

$$\frac{\omega_n^2}{s^2 + 2\zeta\omega_n s + \omega_n^2}$$

$$F(s) = \frac{K_i}{s^2 + 2\zeta\omega_n s + \omega_n^2} \tag{15}$$

The similarities between equation (14) and equation (15) are apparent. The step function response for the frequency control can be written in terms of the impulse response of the function in equation (14) as

$$F(s) = C(s) \frac{K_i}{\omega_n^2}$$

The frequency of this system as a function of $\omega_n t$ can therefore be represented by the curves of Figure 5 if the abcissa is multiplied by K_i/ω_n^2. These curves suggest that the frequency will reach some maximum value and then eventually decay to zero depending on the value of ζ and ω_n.

As stated before, the purpose of the frequency control is the reduction of frequency deviations due to step changes in alternator load. The maximum excursion of the output frequency can be specified as a fraction of the design frequency. If F_o is the design frequency and α the accuracy of control required, then

$$f(t)_{max} = \alpha F_o$$

Finding an expression for $f(t)_{max}$ from equation (13) for $f(t)$ and equating that to αF_o allows for the determination of ω_n as a function of ζ. Once this is done, K_c and Z_o can be found as functions of ζ.

Upon taking the derivative of equation (13) and setting this derivative equal to zero, t_{max} is found as shown in Appendix IV to be

$$t_{max} = \frac{\theta}{\omega_n(\zeta^2 - 1)^{1/2}}$$

where

$$\theta = \cosh^{-1}\zeta$$

Substituting this value into equation (13) gives $f(t)_{max}$.

$$f(t)_{max} = \frac{K_p K_i}{\omega_n} e^{-\zeta\theta/(\zeta^2-1)^{1/2}}$$

Now,

$$\alpha\bar{F}_o = \frac{K_p K_i}{\omega_n} e^{-\zeta\theta/(\zeta^2-1)^{1/2}}$$

or

$$\omega_n = \frac{K_p K_i}{\alpha F_r} e^{-\zeta\theta/(\zeta^2-1)^{1/2}} \tag{16}$$

It was shown earlier that ζ and ω_n were both functions of K_c, the gain of the compensation network, and Z_o, the zero of the compensation network. By rearranging equations (11) and (12) and substituting equation (16) for ω_n, K_c and Z_o are found to be

$$K_c = \frac{2\zeta K_p}{\alpha F_r} e^{-\zeta\theta/(\zeta^2-1)^{1/2}} \tag{17}$$

$$Z_o = \frac{K_p K_i}{2\zeta\alpha F_r} e^{-\zeta\theta/(\zeta^2-1)^{1/2}} \tag{18}$$

Now by specifying α, $\bar{F}_o$, and ζ, the quantities ω_n, K_c, and Z_o can be calculated and f(t) can be plotted as a function of time. Using the values obtained for K_c and Z_o, one can design an electronic circuit for representing $G_c(s)$. This network, an appropriate frequency sensor, and the parasitic load form the complete speed control.

CHAPTER III

DESIGN OF THE COMPENSATION NETWORK

In Chapter II a transfer function that provides for a change in operational load with an opposite change in parasitic load was developed. An electronic circuit to represent this function must use the error signal from the frequency sensor as an input and must produce an output that is proportional to the needed parasitic load. In general, circuits involving dc amplifiers and passive R-C networks are suitable for this application. For this study the compensation network shown in the simplified schematic diagram of Figure 6 was designed.

An operational amplifier rather than another type of dc amplifier was chosen for use in the compensation network for these reasons:

1. The high open-loop gain, high input impedance and low output impedance of the operational amplifier allows for easy representation of the transfer function by the proper choice of passive elements in the input and feedback impedances.

2. The operational amplifier is smaller in size and weight, is less expensive, and consumes less power than available competing devices.

Of the operational amplifiers available, a monolithic operational amplifier was chosen because it offers in general, with the possible exception of chopper-stabilized operational amplifiers, a lower drift rate. Although drift, arising as a result of the finite input offset

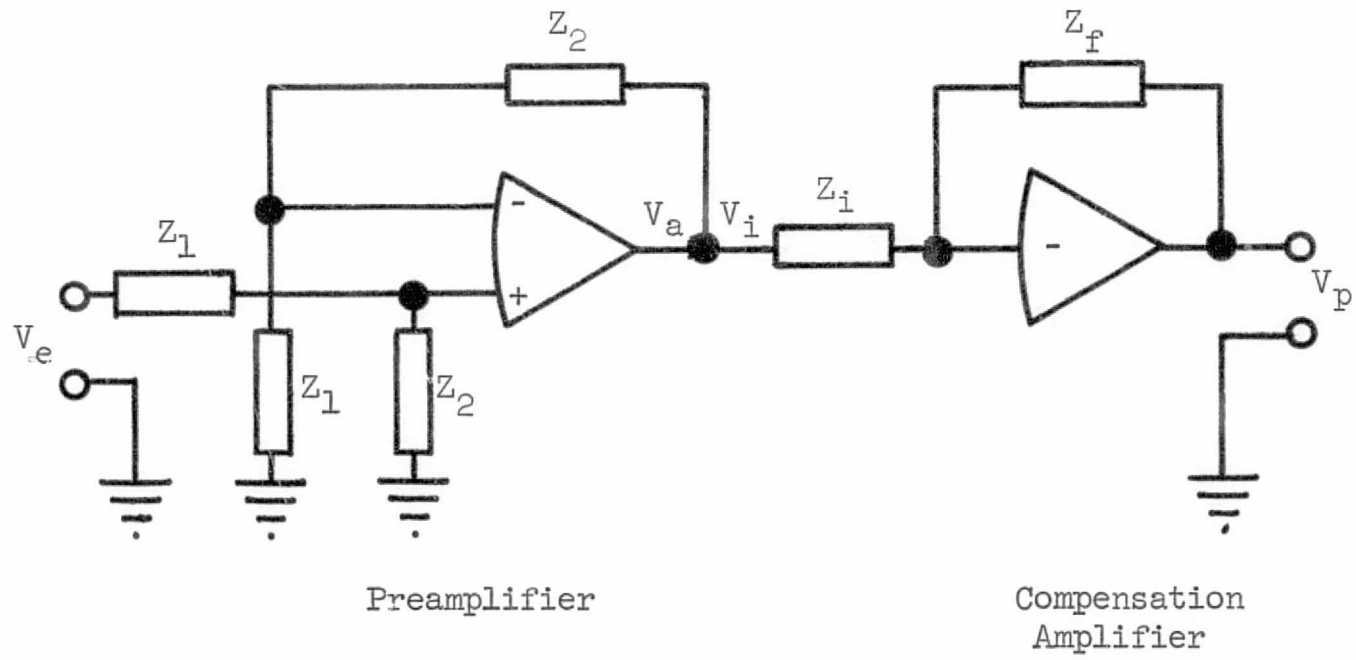

Figure 6.- Simplified schematic diagram of the compensation network

voltage and current, was of little significance in this study, for long-term missions it will become of considerable importance. For these missions one would need to study in detail the drift characteristics of specific amplifiers before making a selection.

Because the gain characteristic of most dc amplifiers roll off faster than 12 decibels per octave, some problems in stability were expected. This disadvantage is generally corrected in integrated circuit operational amplifiers by using an external compensation network for modifying the gain of the amplifier. Usually this is done with resistors and capacitors. This, of course, means that some of the reasons for choosing the integrated amplifier in the first place, namely small size, weight, and expense, are somewhat diminished.

The specific monolithic operational amplifier chosen for this study was the LM 201 made by National Semiconductor Corporation. Information concerning the characteristics of this amplifier is given in Appendix V.

Other components in the compensation network of Figure 6 were determined by analyzing the transfer function of the circuit in terms of the input and feedback impedances. As shown in Appendix VI, the transfer function of the circuit can be written

$$\frac{V_p}{V_e} = -\frac{Z_2}{Z_1}\frac{Z_f}{Z_i}$$

where V_e is the input voltage proportional to frequency error and V_p is the output voltage proportional to the parasitic load required to reduce the frequency error to zero. The input impedances of the

preamplifier and compensation amplifier are Z_1 and Z_i respectively. The feedback impedances are, in the same order, Z_2 and Z_f. As is also shown in Appendix VI, equating V_p/V_e to $G_c(s)$ allows for the development of networks for Z_i and Z_f. The input impedance can be represented by a single resistor, R_i, whereas the feedback impedance can be represented by a series R-C network.

$$Z_i = R_i$$

$$Z_f = R_f + \frac{1}{sC_f}$$

For use in these equations, values for R_f and C_f were determined from the following relationships:

$$R_f = \frac{R_i K_c}{A}$$

$$C_f = \frac{A}{R_i K_c Z_o}$$

where A, the gain of the preamplifier, can be represented by the ratio of the feedback to input impedances with single resistors as the impedances.

$$A = \frac{Z_2}{Z_1} = \frac{R_2}{R_1}$$

Before A, R_f, and C_f can be calculated, K_c and Z_o must be determined. Both of these quantities were shown in Chapter II to be functions of ζ, which is the damping ratio for the system, and α, which is the maximum change in frequency that can be tolerated. The proper values of ζ and α can be chosen by determining the system response for

several values of ζ and α, and by then picking the response that best meets the frequency specifications.

Now, the question arises as to what would be reasonable ranges of values for α, ζ, and t. In an operational dynamic power system the maximum excursion of the output frequency will be dictated by power requirements. At the present time loads for spacecraft that will use dynamic power systems are not defined well enough to generate accurate frequency specifications. Based on experience with prototype life-support equipment and controlled-moment-gyro attitude control equipment, maximum frequency deviations of as much as 5 per cent can be tolerated. Although most of these loads would operate more effectively with closer frequency control, little can be gained by controlling frequency deviations below 1 per cent. Thus, a practical range of values of α for the parasitic-load speed control appears to be from 1 per cent to 5 per cent.

The effect of variations in ζ on K_e and Z_o is difficult to ascertain from equations (17) and (18). These values must therefore be calculated for a wide range of ζ's. From Figure 5 one sees that sinusoidal variations are damped out very slowly for ζ's of 0.1 or less. For ζ's greater than 1 no oscillations occur but the rate of closure to the initial value of frequency is slower. A reasonable choice for ζ should therefore be in the range of 0.1 to 1.0.

Since most loads respond slowly to changes in frequency, a control system that returns the frequency to within 1 per cent of the design value in 1 second or less can be tolerated. Therefore, the

frequency was plotted for times ranging from 0 to 3 seconds to give an adequate indication of the response.

The frequency response for a step load change, K_c, was found in Chapter II as

$$f(t) = \left[\frac{K_p K_i}{\omega_n(\zeta^2-1)^{1/2}}\right] e^{-\zeta\omega_n t} \sinh\left[\omega_n(\zeta^2 - 1)^{1/2} t\right]$$

For a given dynamic power system, K_p will be defined. From the following equation, K_i can be calculated.

$$K_i = \frac{p^2}{21.7\pi^2 J F_o} \tag{19}$$

where p, J, and F_o will also be defined by the design of the power system. Values of ω_n can be calculated from equation (16) for a given value of ζ and α. Once these values are known for a given ζ and α, f(t) can be calculated for different values of time.

The digital computer program shown in Appendix VIII was written for determining values of K_c, Z_o, and ω_n for any value of ζ and α. For use in this program, K_p, p, J, and F_o were chosen from the specifications of a preliminary design of a radioisotope Brayton-cycle space power system by McDonnel-Douglas Company.[8] The maximum load expected for this system was 11 kilowatts; the design frequency was 1067 hertz. For simplicity 10 kilowatts and 1000 hertz were used in the program. By using the F_o of 1000 hertz, the number of poles on the alternator

---

[8] G. G. McKhann, "Preliminary Design of Pu-237 Isotope Brayton-Cycle Power System for MORL" (Santa Monica, California), IV, I-213.

as 2, and the inertia of the CRU as 0.001 slug-feet, K_i was calculated from equation (19) to be 0.0187.

The values for K_c, Z_o, and ω_n that resulted from the digital computer program for ζ's ranging from 0.1 to 1.0 and α's ranging from 0.01 to 0.05 are listed in Table 1. Using these data, one can plot the exact output frequency as a function of time for a disturbance in alternator load. This presentation is given in Figure 7.

From these curves one can see that the output frequency change will be less than 1 per cent of the design value in 1 second only for maximum deviations of less than 4 per cent. For an α of 0.03 any ζ between 0.4 and 0.6 will give this response. By using a ζ of 0.6, frequency oscillations can be minimized. Table 1 shows that for an α of 0.03 and a ζ of 0.6, K_c is 199.5 and Z_o is 2.6.

These values of K_c and Z_o can now be used for calculating A, R_f, and C_f. Values for R_1 and R_i were chosen as 10 kilohms, as suggested by the amplifier manufacturer, to minimize input offset voltage, thereby decreasing output error. Now, C_f becomes

$$C_f = \frac{A}{(10^4)(199.5)(2.6)}$$

$$= \frac{A}{5.2 \times 10^6} \qquad (20)$$

TABLE 1.- VALUES OF K_c, Z_o, AND ω_n

α	ζ	K_c	Z_o	ω_n
0.01	0.1	172.5	80.3	16.0
	0.2	302.4	35.2	14.1
	0.3	402.9	20.8	12.5
	0.4	482.3	14.0	11.2
	0.5	546.3	10.2	10.2
	0.6	598.6	7.7	9.3
	0.7	642.0	6.1	8.5
	0.8	678.4	4.9	7.9
	0.9	733.5	4.1	7.3
	1.0	735.8	3.4	6.8
0.02	0.1	86.2	40.1	8.0
	0.2	151.2	17.6	7.0
	0.3	201.5	10.4	6.2
	0.4	241.2	7.0	5.6
	0.5	273.1	5.1	5.1
	0.6	299.3	3.9	4.6
	0.7	321.0	3.0	4.3
	0.8	339.2	2.5	3.9
	0.9	354.6	2.0	3.7
	1.0	367.9	1.7	3.4
0.03	0.1	57.5	26.8	3.7
	0.2	100.8	11.7	4.7
	0.3	134.3	6.9	4.2
	0.4	160.8	4.7	3.7
	0.5	182.1	3.4	3.4
	0.6	199.5	2.6	3.1
	0.7	214.0	2.0	2.8
	0.8	226.1	1.6	2.6
	0.9	236.4	1.4	2.4
	1.0	245.2	1.1	2.3

TABLE 1.- Concluded.

α	ζ	K_c	Z_o	ω_n
0.04	0.1	43.1	20.0	4.0
	0.2	75.6	8.8	3.5
	0.3	100.7	5.2	3.1
	0.4	120.6	3.5	2.8
	0.5	136.6	2.5	2.5
	0.6	149.6	1.9	2.3
	0.7	160.5	1.5	2.1
	0.8	169.6	1.2	2.0
	0.9	177.3	1.0	1.8
	1.0	183.9	0.9	1.7
0.05	0.1	34.5	16.0	3.2
	0.2	60.5	7.0	2.8
	0.3	80.6	4.2	2.5
	0.4	96.5	2.8	2.2
	0.5	109.2	2.0	2.0
	0.6	119.7	1.5	1.9
	0.7	128.4	1.2	1.7
	0.8	135.7	1.0	1.6
	0.9	141.9	0.8	1.5
	1.0	147.2	0.7	1.4

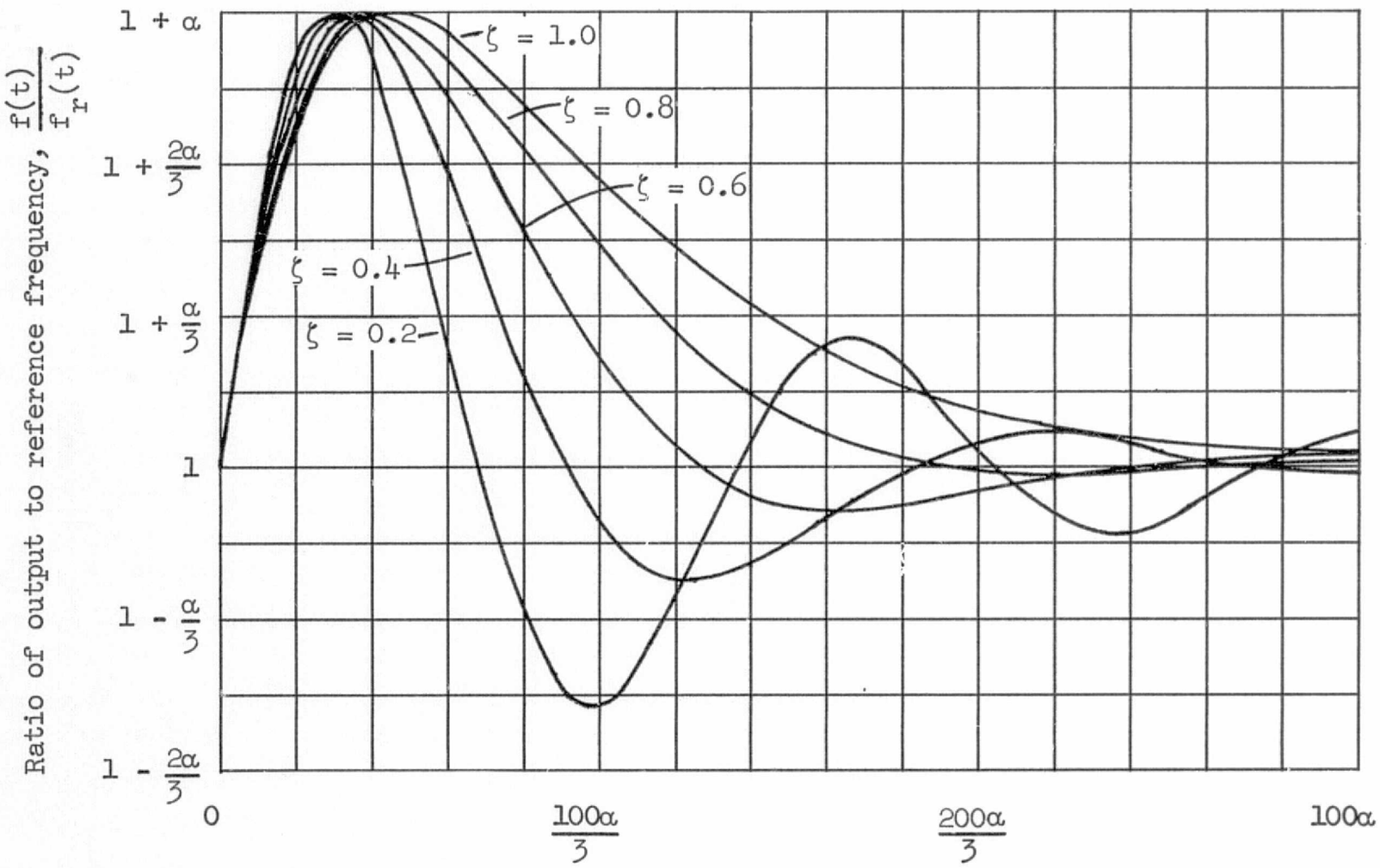

Figure 7.- Theoretical frequency response of the control system for a 10kW step decrease in load

and R_f becomes

$$R_f = \frac{(10^4)(199.5)}{A}$$

$$= \frac{1.995 \times 10^6}{A}$$

From these two equations, one sees that C_f is proportional to A and R_f is inversely proportional to A. Since the error in the gain of the operational amplifier increases with increased R_f, R_f should be kept small. This means C_f must be large. Capacitors with close tolerances, good stability, and small size can be obtained for values up to around 1 microfarad. If 1 microfarad is used as the value for C_f, the gain of the preamplifier can be calculated from equation (20) as

$$A = (5.2 \times 10^6)(10^{-6})$$

$$= 5.2$$

and R_f will be

$$R_f = \frac{1.995 \times 10^6}{5.2} \ \Omega$$

$$= 384 \ k\Omega$$

The feedback impedance for the preamplifier can be calculated from the relationship for the gain of the preamplifier.

$$R_2 = AR_1$$

$$R_2 = 5.2 \times 10^4 \ \Omega$$

$$= 52 \ k\Omega$$

The transfer function for the compensation circuit now becomes

$$G_c(s) = -\left(199.5 + \frac{518.7}{s}\right)$$

$$= -199.5\left(\frac{s + 2.6}{s}\right)$$

The networks for Z_1, Z_i, and Z_f were combined with the operational amplifier and its associated circuitry in the complete compensation network of Figure 8. Values for the stabilization capacitors C_1 and C_2 and the balancing resistors R_3, R_4, R_5, and R_6 were suggested by the amplifier manufacturer (See Appendix V).

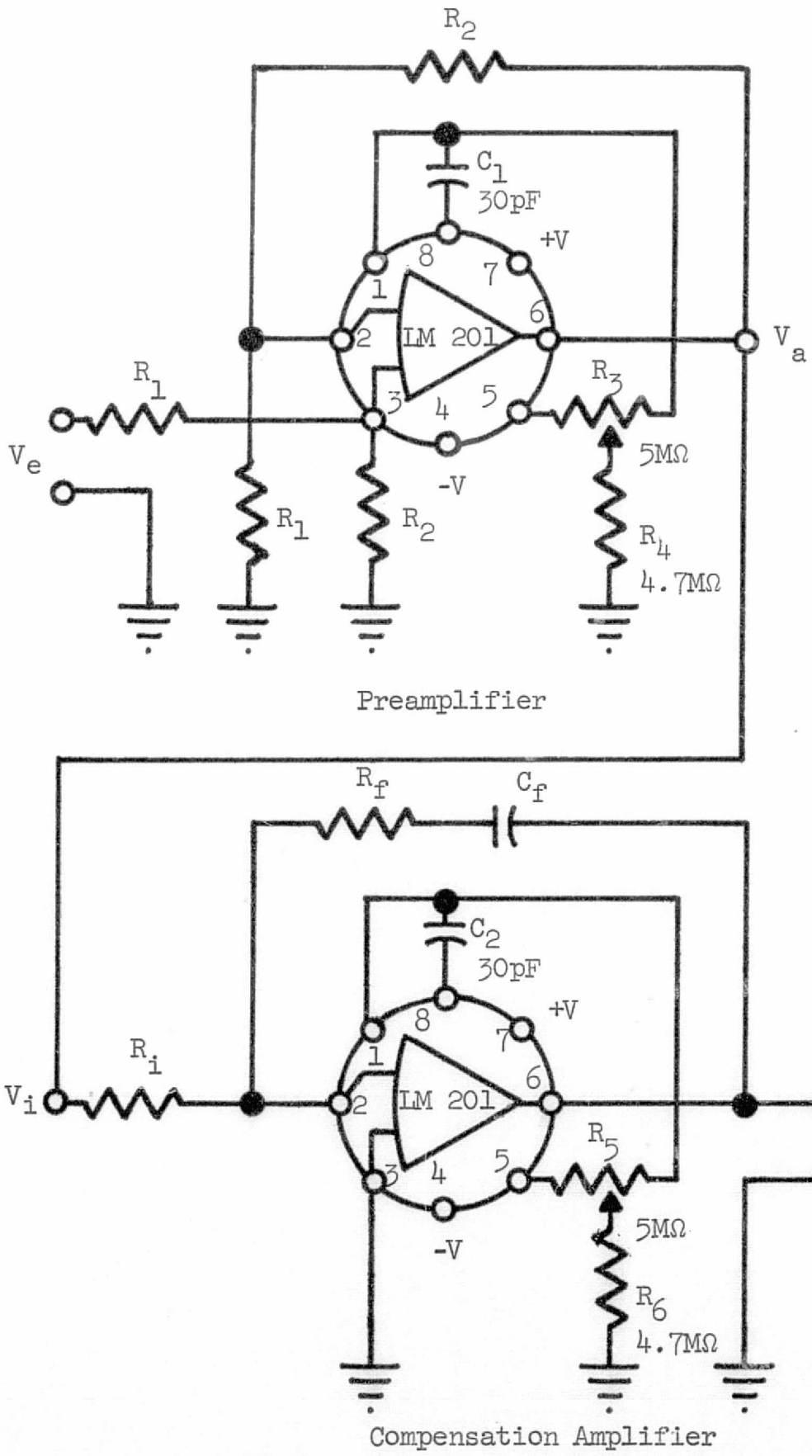

Figure 8.- Schematic diagram of compensation netwórk

CHAPTER IV

EXPERIMENTAL PROCEDURES

For determining the operational characteristics of the speed control, the compensation network developed in Chapter III was used along with analog simulations of the CRU, frequency detector, and parasitic load. The logic diagram for this study is shown in Figure 9.

The transfer function of the CRU is given by

$$\frac{F(s)}{P_{sh}(s) - P_l(s) - P_p(s)} = \frac{K_i}{s}$$

where K_i was previously calculated to be 0.0187. Although this function is a simple integration, the time constant is so large that simulation with one operational amplifier is impractical. Thus, two amplifiers, A4 and A5, for attenuating the signal and an integrator, I, were used in the simulation. Amplifier A4 summed the three input values, $P_{sh}(s)$, $P_l(s)$, and $P_p(s)$, and attenuated these inputs with a gain of 0.100. Amplifier A5 further attenuated the input signal with a gain of 0.187. It was then possible to use an integrator, I, with a time constant of 0.100 to give an output of the CRU simulation that was 10 times the negative of the alternator frequency.

The frequency detector, which compares the output frequency to a reference frequency and gives an output proportional to the difference of the two, was simulated with a summing amplifier. A voltage

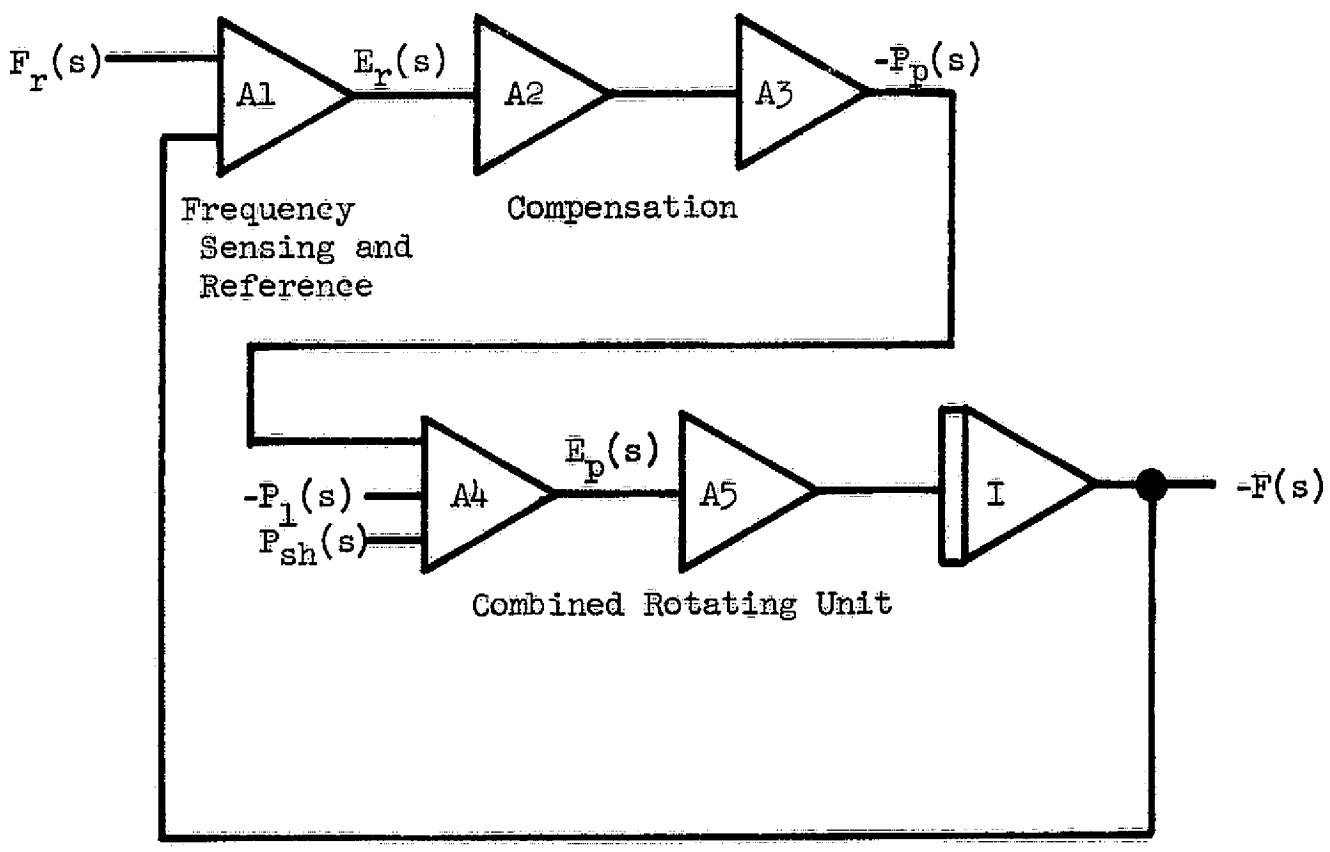

Figure 9.- Logic diagram for analog studies

proportional to the alternator frequency was available from integrator I. Amplifier A1 attenuated this voltage with a gain of 0.1 and summed it with a reference voltage. The output from A1 was therefore $-\left[f_r(t) - f(t)\right]$.

The output of A5 was then used as the frequency error signal required by the compensation network. Since the output of the network is a linear function of the parasitic load, the output of this network could be used as the parasitic power input for A4 to complete the loop.

This experimental setup, pictured in Figure 10, was used to study the response of the speed control under four conditions of loading that are expected to occur in actual operation. With a reference frequency of 1000 hertz and a fixed mechanical input, the output frequency and output of the compensation network, as functions of time, were determined for addition and removal of the total operational load of 10 kilowatts. This type of load change will occur only in start-up, shut-down, and emergency conditions. The same parameters were determined for addition and removal of the total load in steps of 2 kilowatts, which is representative of the more normal operating conditions. The output of the compensation network, being directly proportional to the parasitic load, was used to size the parasitic load required to properly regulate the output frequency. The experimental setup was also used to study the response of the output frequency to changes in the reference frequency.

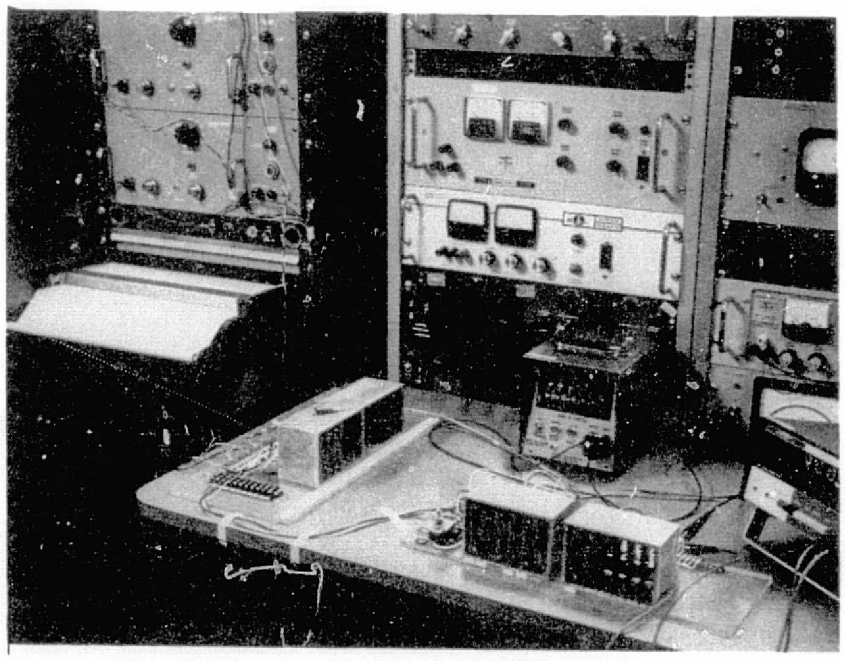

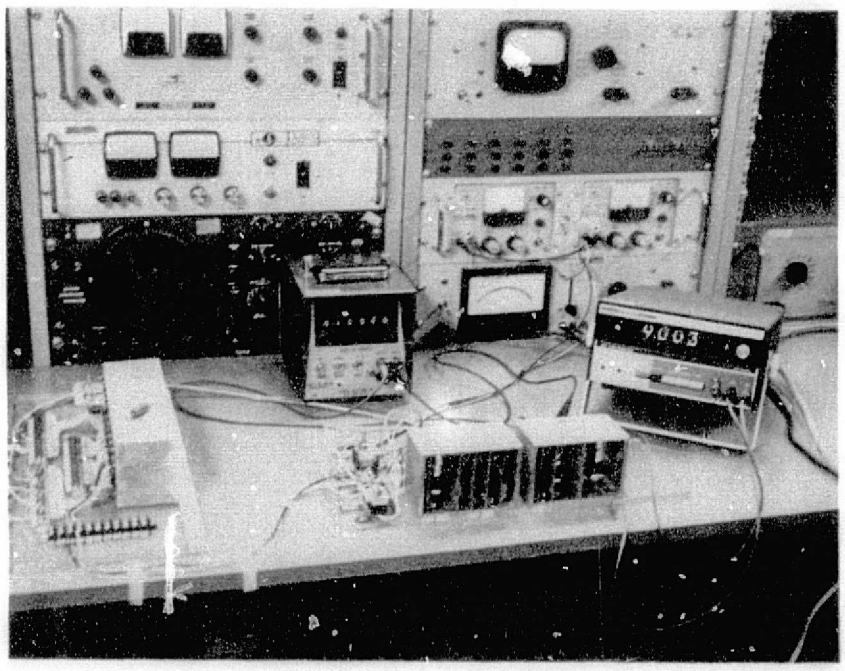

Figure 10.- Photographs of experimental setup

CHAPTER V

RESULTS

Figure 11 shows the output frequency and parasitic load as functions of time for addition of the operational load in one step. Figure 12 presents the same parameters for removal of the load. These conditions, which are expected to occur only in isolated cases, represent the greatest load disturbances and produce the worst deviations in frequency.

The frequency plot of Figure 12 is the inverse of that of Figure 11. Both plots compare favorably with the theoretical plot of Figure 7 for an α of 0.03 and a ζ of 0.6. In both cases, the control returns the frequency to within ± 1 per cent of the design frequency in 1 second or less. The traces for the parasitic load show that a maximum of 13.2 kilowatts must be removed or added momentarily to return the frequency to its original value. Since 3.2 kilowatts are used in each case only to reverse the acceleration of the CRU, the final change in the parasitic load is equal to the total change in operational load. In the case of addition of operational load, 3.2 kilowatts must remain connected to the alternator to keep the parasitic load from going negative.

For an indication of the response of the control system under more normal load changes, data were obtained for addition and removal of the load in five steps of 2 kilowatts. These data are shown in

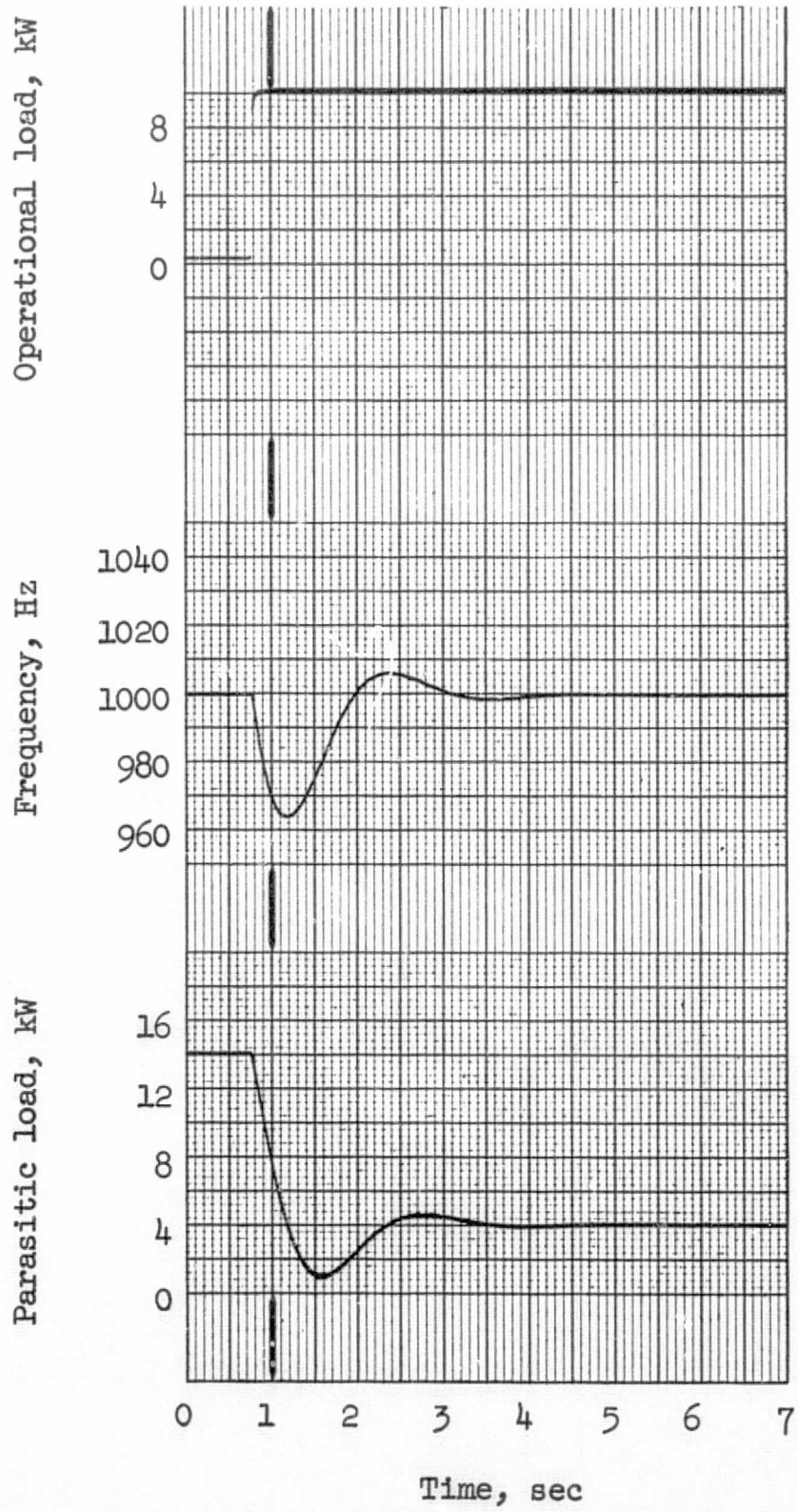

Figure 11.- Frequency and parasitic load responses for addition of a 10kW load

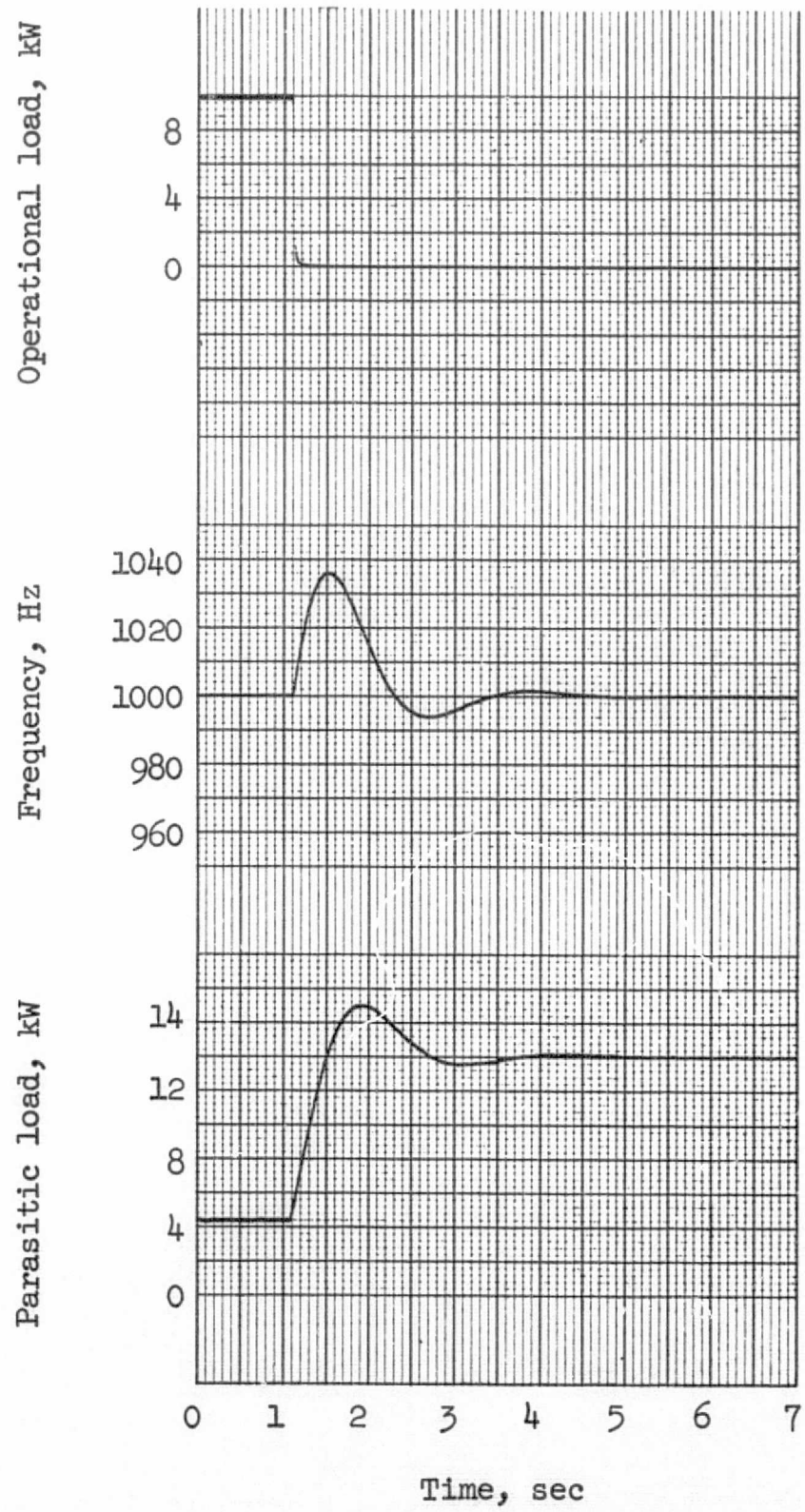

Figure 12.- Frequency and parasitic load responses for removal of a 10kW load

Figures 13 and 14. It is apparent that these curves can be obtained directly from Figures 11 and 12 by an appropriate change of scale. The maximum deviation in frequency for each step is 20 per cent of that for the full load step. The parasitic load response is equal to the load step with a momentary overshoot of 30 per cent of the step change. This overshoot is approximately the same percentage as was experienced for the full load changes. In the case of addition of operational load, 0.6 kilowatt must remain connected to the alternator to prevent the parasitic load from going negative when the last 2 kilowatts of load are added.

Since the parasitic load represents most of the size and weight of the control system, it is desirable to carry only the amount of load that will meet both normal and unusual load changes. To determine the load needed for conditions of full load changes, the parasitic load plots of Figures 11 and 12 can be combined. The total load required will be equal to the total load removed plus the sum of the overshoot needed when load is added and the overshoot needed when load is removed. The total parasitic load for this condition will be 16.4 kilowatts. As was mentioned before, 3.2 kilowatts will remain connected to the alternator under full operational load conditions.

The total parasitic load required for changes of 2 kilowatts can be determined in the same manner from Figures 13 and 14. The total load change is 10 kilowatts; the overshoot is 0.6 kilowatt for either addition or removal of load. The size of the parasitic load necessary for control in this case will then be 11.2 kilowatts with 0.6 kilowatt connected to the alternator at all times.

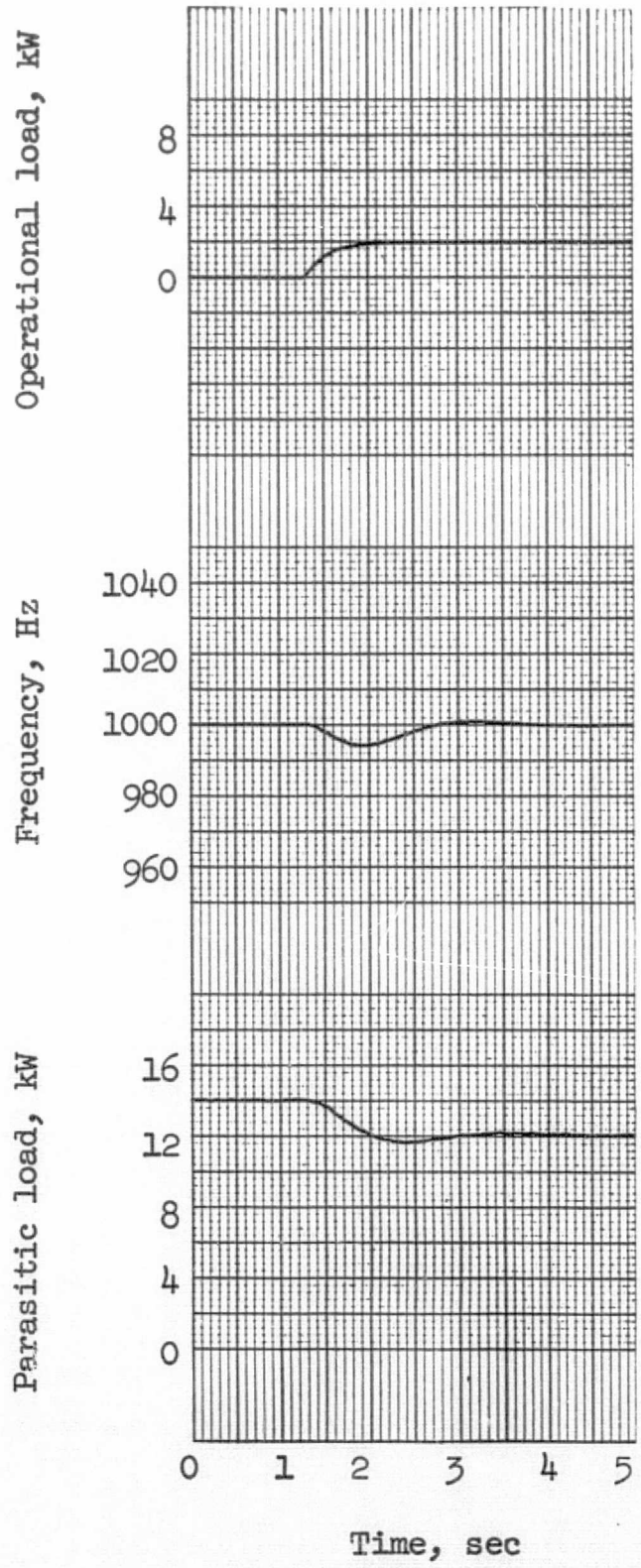

Figure 13a.- Frequency and parasitic load response for addition of a 10kW load in 2 kW increments

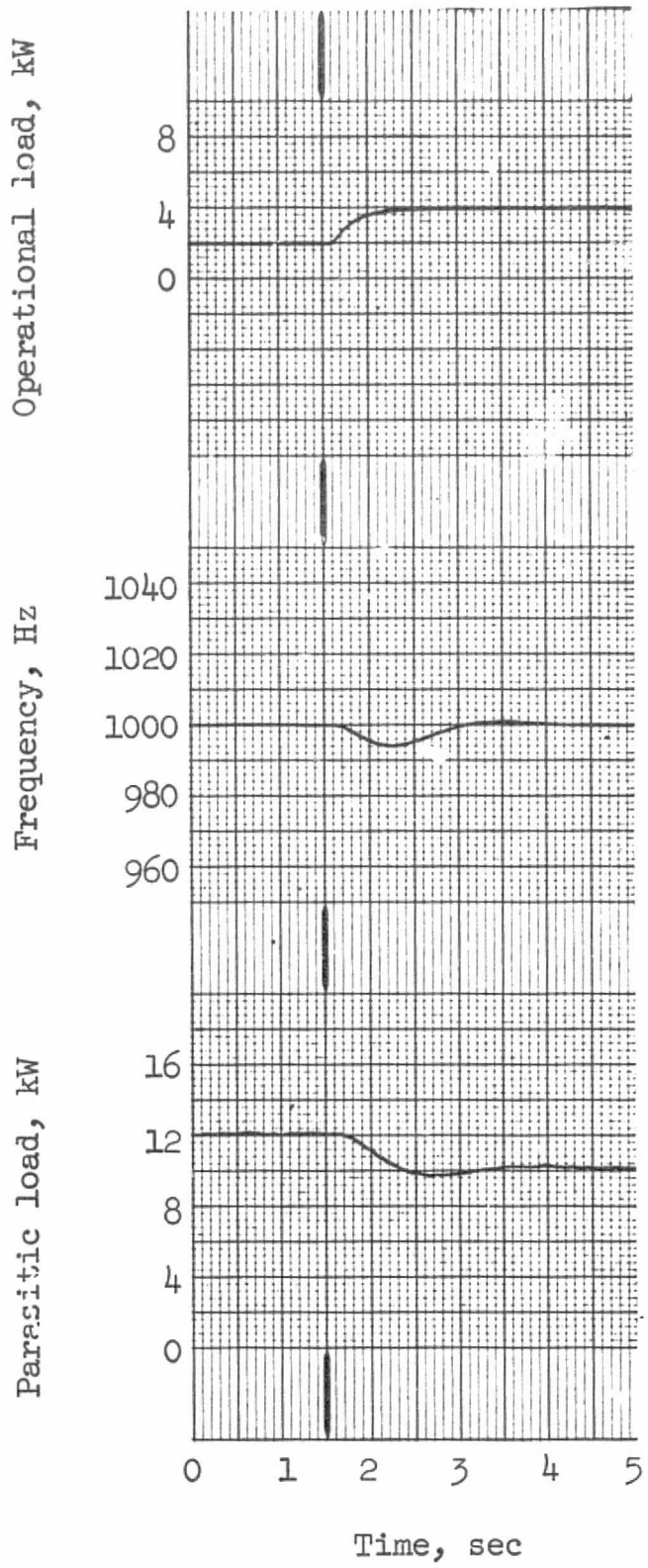

Figure 13b.- Frequency and parasitic load response for addition of a 10kW load in 2kW increments

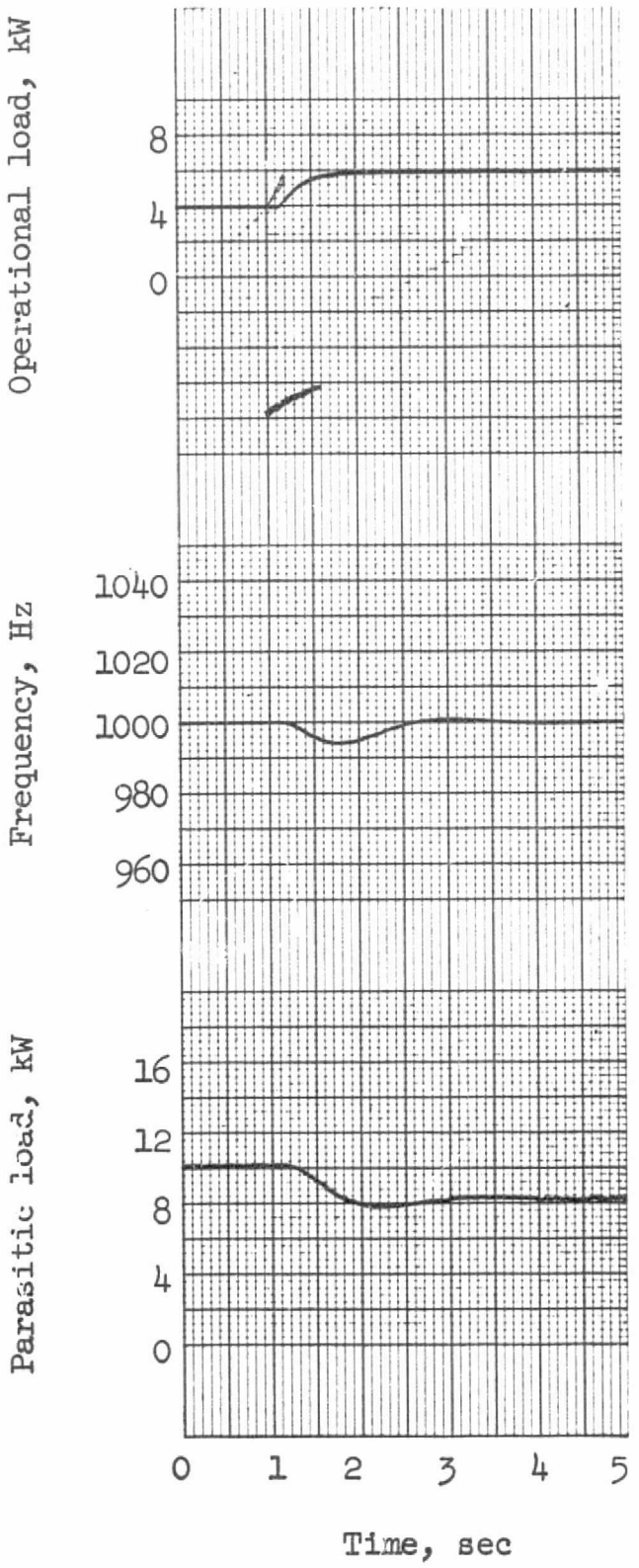

Figure 13c.- Frequency and parasitic load response for addition of a 10kW load in 2kW increments

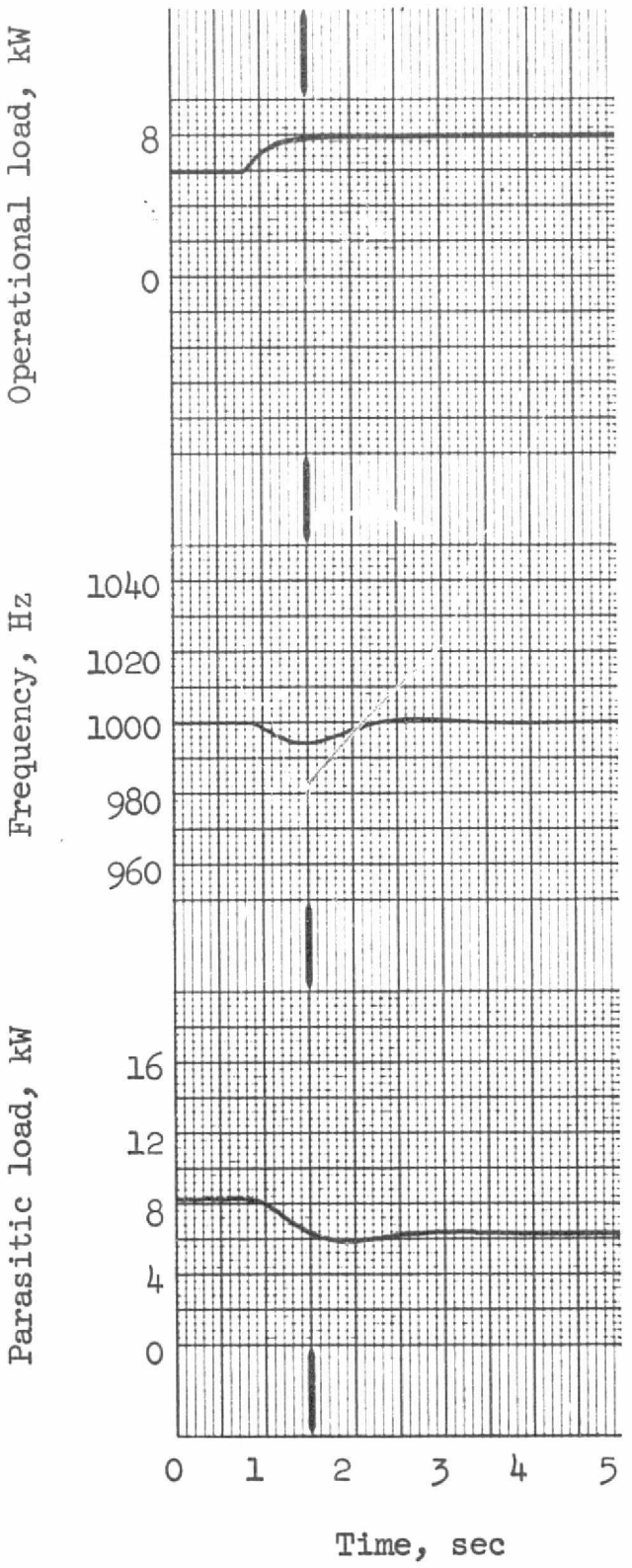

Figure 13d.- Frequency and parasitic load response for addition of a 10kW load in 2kW increments

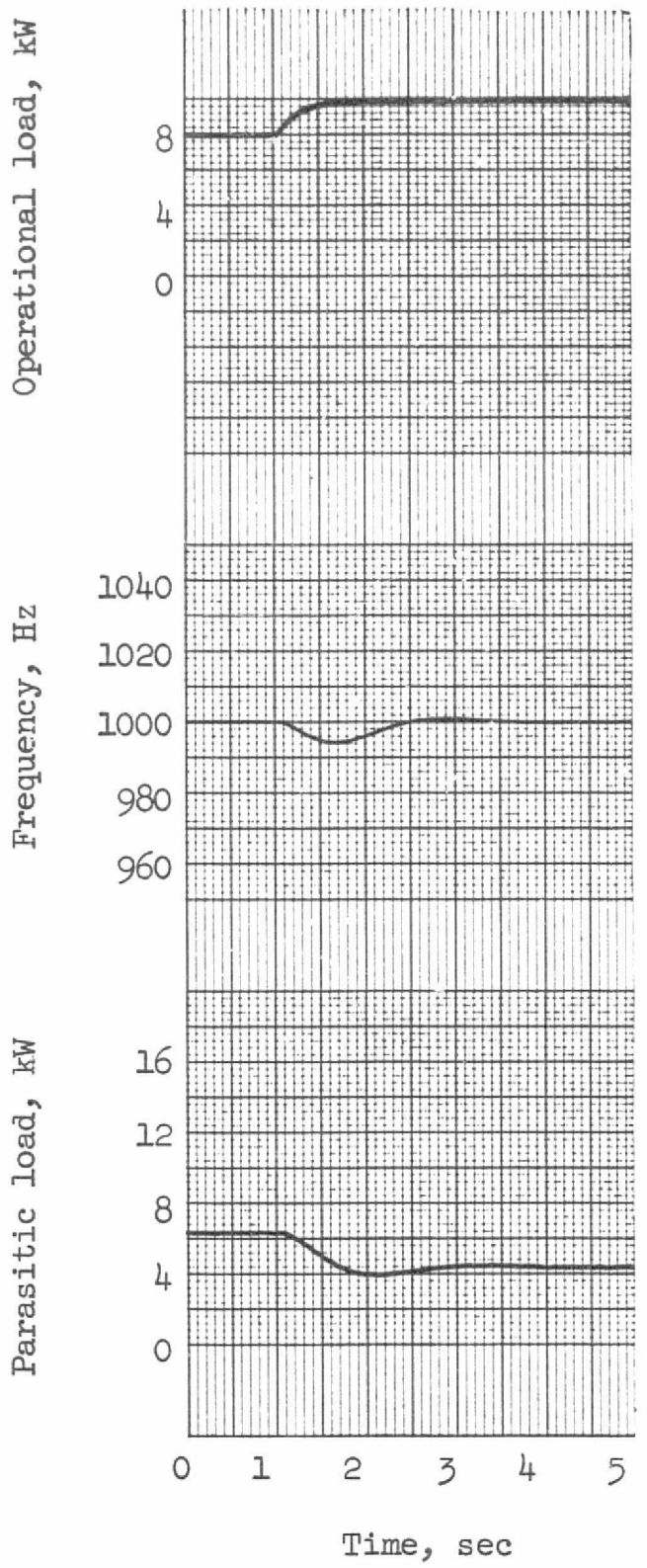

Figure 13e.- Frequency and parasitic load response for addition of a 10kW load in 2kW increments

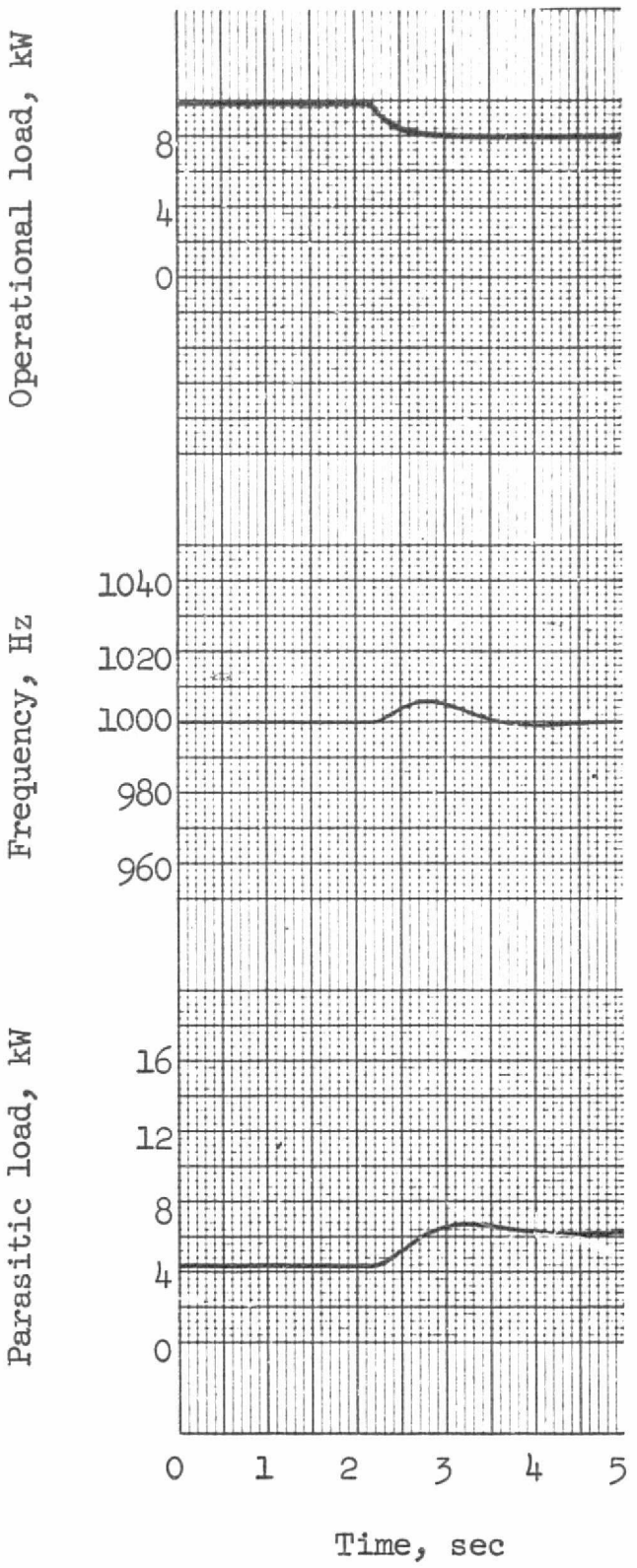

Figure 14a.- Frequency and parasitic load response for removal of a 10kW load in 2kW increments

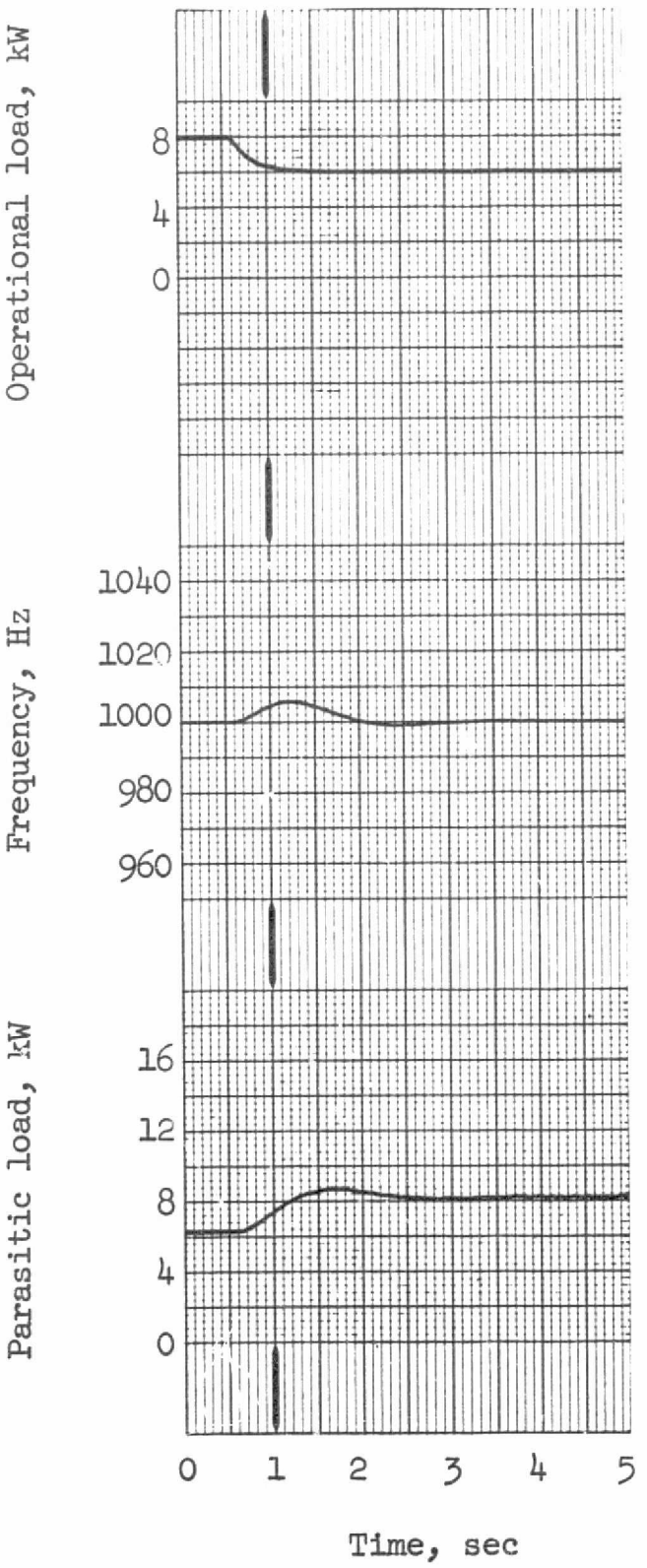

Figure 7b.- Frequency and parasitic load response for removal of a 10kW load in 2kW increments

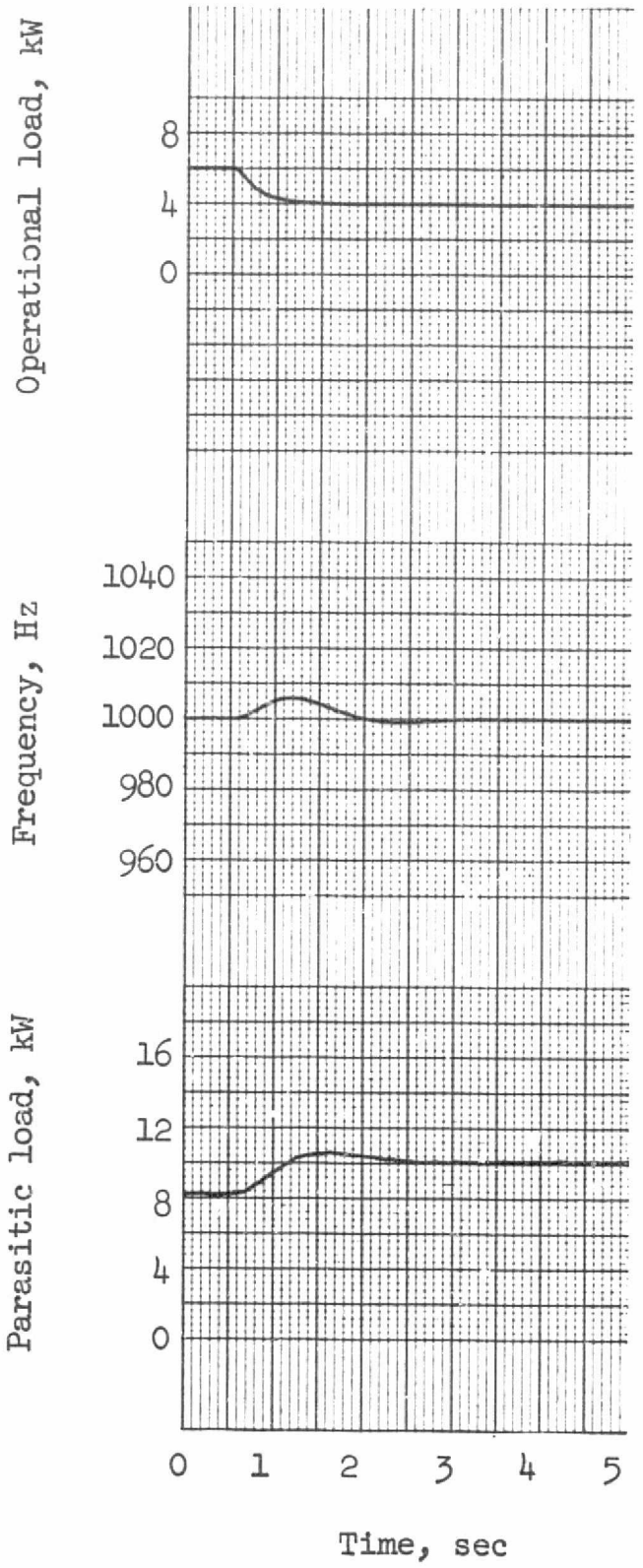

Figure 14c.- Frequency and parasitic load response for removal of a 10kW load in 2kW increments

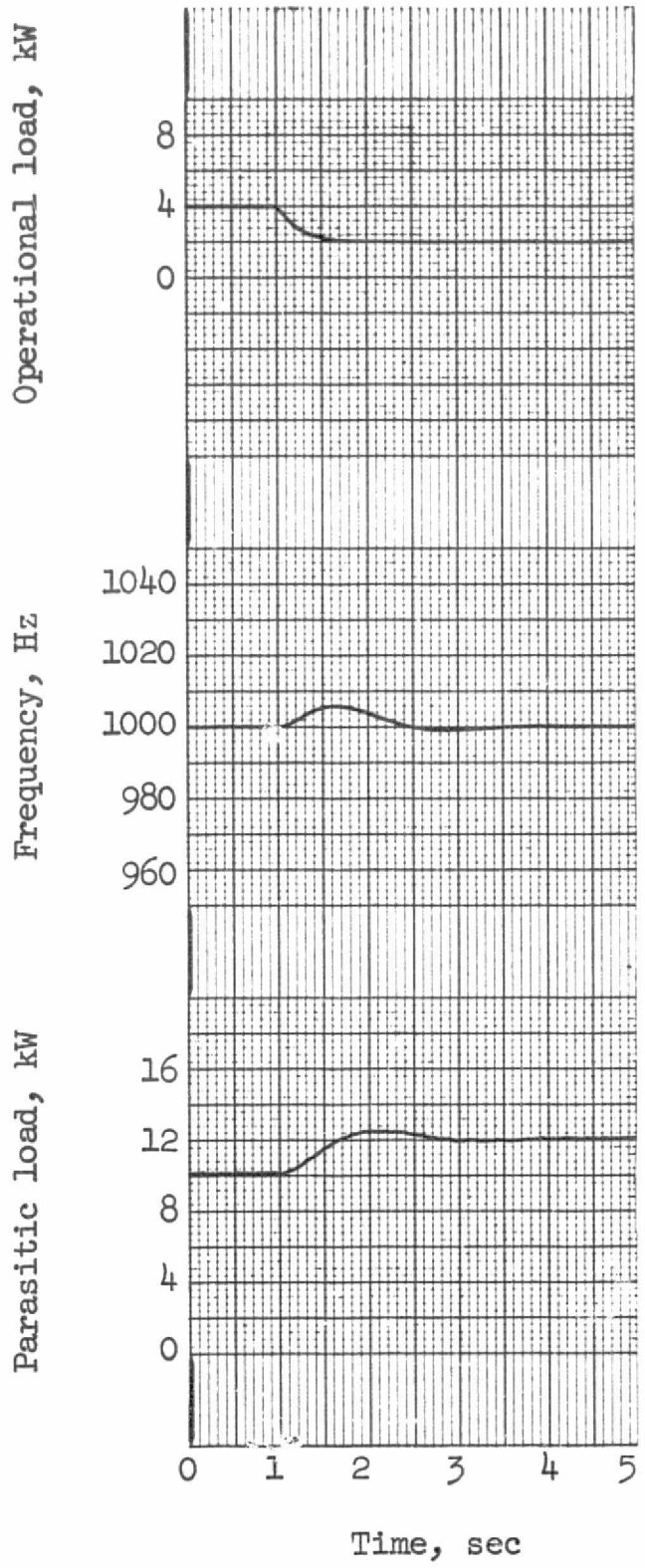

Figure 14d.- Frequency and parasitic load response for removal of a 10kW load in 2kW increments

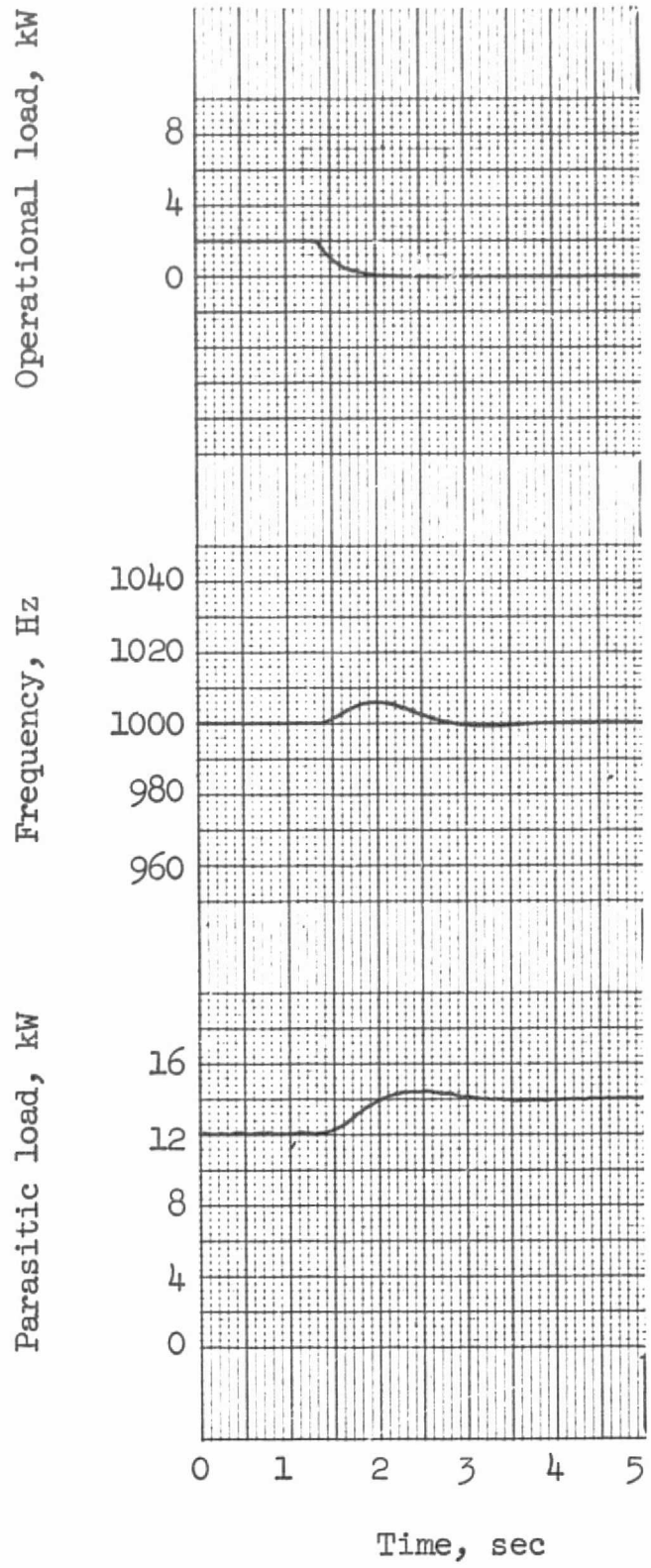

Figure 14e.- Frequency and parasitic load response for removal of a 10kW load in 2kW increments

For this control the minimum size of parasitic load that will maintain control to ±1 per cent of the design frequency in 1 second or less under all conditions of loading is 16.4 kilowatts. This load is 64 per cent larger than the maximum operational load. To carry this much parasitic load might be objectional from a size-and-weight standpoint. The parasitic load could be reduced by relaxing slightly the frequency specification for the full load changes. Since these changes are expected to occur only in conditions where frequency control to the set limits might not be necessary, this would appear to be a practical alternative. For this particular control, one sees from Figure 11 that 10 kilowatts of parasitic load will reduce the acceleration of the CRU to zero and will maintain a frequency error of -3 per cent. A parasitic load that is slightly larger than 10 kilowatts will insure that the frequency returns to -1 per cent of the design frequency although the time required will be longer than 1 second. Thus, for this particular control, the load established for step changes of 2 kilowatts, 11.2 kilowatts, would also handle full load changes if the time in which the frequency returns to the design frequency is increased.

The excess parasitic load that must remain on the alternator to prevent the load from going negative represents an uneconomical use of energy since this power cannot be used for any other purpose. This additional power requirement can be eliminated by designing the control for zero parasitic load under full operational load conditions. Under these circumstances, when the full load is added the control would call for enough negative load to restore the system to equilibrium. Since

this negative load, which can be interpreted as an energy demand on the system, is momentary, some of the operational loads could be switched off long enough to restore equilibrium. However, since the amount of load that must be removed will vary and since the time that the load must remain off is critical, this method is not practical. A more acceptable method would be to use batteries, which will normally be part of the power system to take care of start-ups and peak loads, for supplying the extra energy. The batteries can be operated in conjunction with a dc bus that is supplied from the alternator. One method for dividing the load properly between the alternator and the batteries involves supplying energy to the dc bus from the alternator through a voltage regulator and from the battery through a current regulator. Since the signal from the compensation network can be used to control the current regulator, the amount of power delivered from the batteries is proportional to the change in alternator frequency. When power is supplied to the dc bus from the batteries, the bus voltage will begin to increase. To maintain the proper voltage level, the voltage regulator will reduce the amount of energy supplied from the alternator. Thus, the energy supplied by the batteries appears to the alternator as a reduction in load demands or as a negative parasitic load. As a result, system equilibrium will be restored.

Since the control system must also maintain the output frequency equal to a reference frequency, data were obtained for the response of the system to a change in the reference frequency. The results are

shown in Figure 15. The output frequency overshoots the step change by 30 per cent but returns to the final value in less than 3 seconds.

As can be determined from Figures 11 and 12, there is approximately 17 per cent difference between the frequency plots of these figures and the theoretical plot of Figure 7. The frequency plots of Figures 13 and 14, however, show very little difference when compared to the expected results.

Error in the frequency plots can be attributed to several factors. Some error in the gain of the operational amplifier is expected due to the non-ideal characteristics of the amplifier. Additional error in the gain arises as a result of using inputs other than dc. Errors can also result by using components with values that do not match exactly the calculated values. Finally, errors can be introduced by the recording equipment.

Errors due to non-ideal characteristics of the operational amplifier are discussed in an application note of Union Carbide.[9] By using the nomographs presented in this reference and the characteristics of the LM 201, the maximum error for each amplifier in the simulation can be determined. Because of the high open-loop gain and low output impedance of the LM 201 and because of the low closed-loop gains used, the maximum error for any amplifier is 0.001 per cent or less.

---

[9]"Operational Amplifier Static Gain Errors Analysis and Nomographs," Union Carbide Electronics AN-7 (Mountain View, California, 1966).

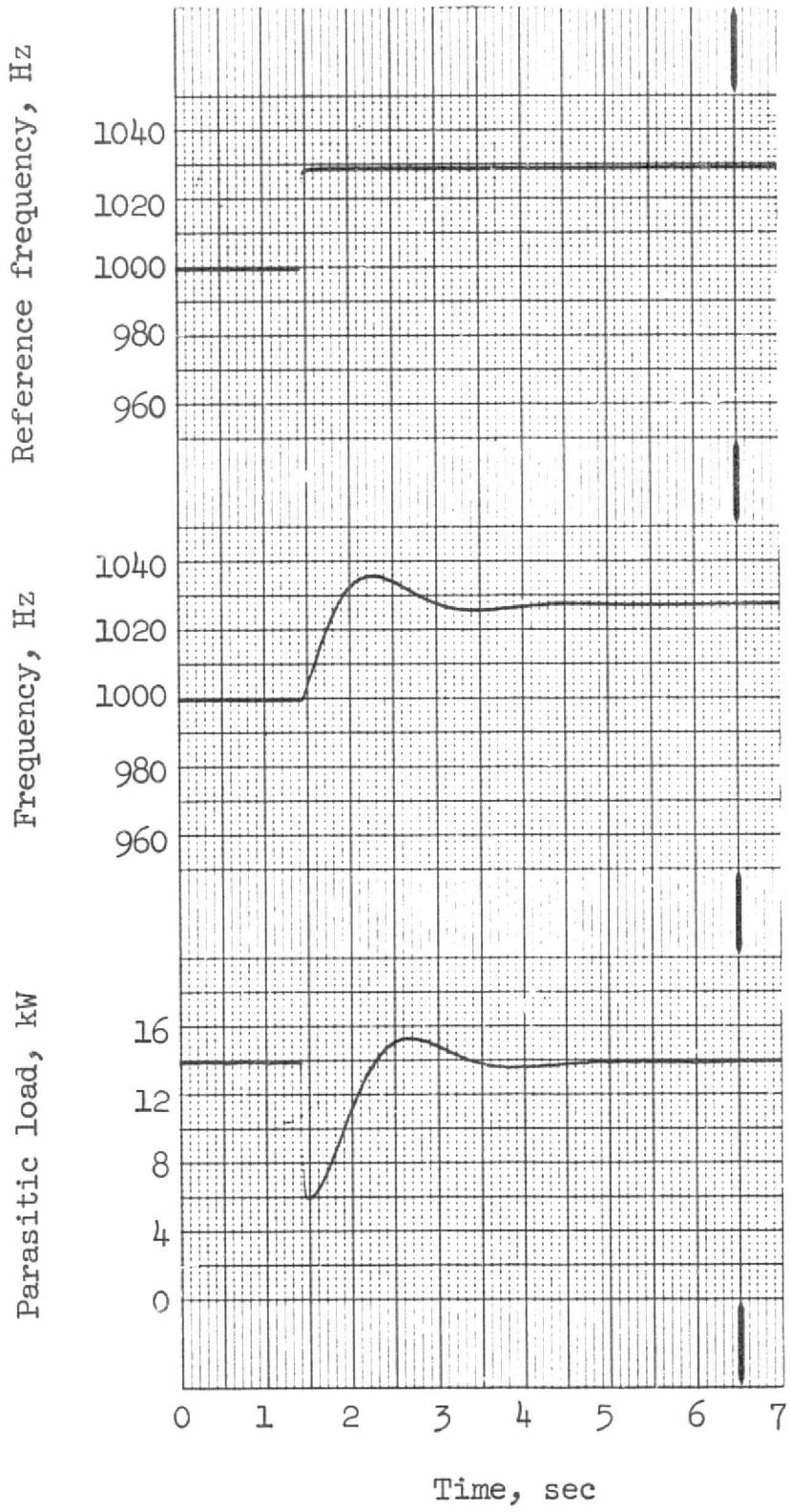

Figure 15.- Frequency and parasitic load responses for a 30Hz increase in the reference frequency

Errors in the gain of the operational amplifier with ac inputs are discussed by Weden.[10] The natural frequency of the system is given in Table 1 as 3.1 radians per second. Since this frequency is less than the frequency at which the gain of the open-loop amplifier starts to roll off, 37 radians per second, no error will be introduced by operation at this frequency.

By using variable gain amplifiers for A1, A4, and A5, the closed-loop gain of these amplifiers was adjusted to within 0.1 per cent. Since components with tolerances of ±1 per cent were used in amplifiers A2, A3, and integrator I, the error introduced by each of these amplifiers will be less than 2 per cent. Thus, from all of these sources the error contributed by the compensation network and simulation is expected to be less than 6 per cent.

During the analog studies, one channel of the recorder exhibited considerable drift and a high noise level. The preamplifier for this channel was replaced but the amplifier had to be frequently recalibrated. Since this channel was used for recording the frequency response, most of the error in the frequency plots of Figures 11 and 12 can be attributed to this source.

Now that the concept of a variable parasitic-load control has been shown feasible, some problems associated with the design of the actual control must be considered. First, the bus for the operational load and the bus for the parasitic load must be arranged independently

---

[10] C. V. Weden, "Operational Amplifier Principles," Orbit (January, 1965), 9-15.

to prevent a fault on one from affecting the operation of the other. The design of the parasitic-load bus must eliminate as completely as possible the likelihood of a fault that might render the control system inoperative. As an added safety factor, circuitry should be included to shut down the power system if for some reason the parasitic-load control does fail or if the error in alternator frequency becomes excessive.

Secondly, frequency sensors must be connected to all three phases of the alternator so that no loss of signal will occur because of an unsymmetrical fault on the system or failure of a sensor. The output of the sensors should be combined to insure that the signal from one will always be available to the control system.

Thirdly, since the parasitic load will consist of dissipative elements, adequate cooling must be provided to maintain the elements at a reasonable operating temperature. This can be accomplished by including a separate radiator for the parasitic load or by using the radiators of the power system or the environmental control system.

Finally, a method for regulating the power to the dissipative elements must be selected. Transistors and silicon controlled rectifiers (SCR's) are suitable devices but each of these devices has certain limitations. The transistor is limited by its low operating power and voltage. The power handling limitations can be eliminated by either splitting the parasitic load into many sections or operating transistors in parallel. The voltage limitations can be eliminated by transforming to a lower voltage and then rectifying.

The SCR is limited for use as a control for the parasitic load for the following reasons:

1. Since the SCR is a switching and not a linear device, large voltage transients are produced when the SCR's are turned on or off. These transients can damage some devices connected to the system and can cause intermittent switching of other SCR's.

2. Radio frequency interference is generated by the rapid rate of change in the current to the load when the SCR is turned on. This RF noise will be present in dc systems and in ac systems when the SCR is switched on at a point where the voltage waveform is other than zero.

3. Automatic commutation does not occur if SCR's are used as switches in dc systems. Additional circuitry must be provided to force the SCR to turn off. The commutation or turn-off circuitry usually involves an additional control device with the same power handling capability of the SCR.

The limitations of the SCR can be minimized by dividing the parasitic load into several sections and using phase control for linear control of a small percentage of the load. Filtering of the transients created by this small section of load can be easily accomplished since the energy involved is small. When the linearly controlled section has been turned fully on, a second section of the same size can be switched on as the linearly controlled section is turned off. By controlling the second section with an SCR that is turned on at zero crossing of the voltage waveform, transients are eliminated. This

process can be repeated until all sections of the parasitic load are on. The reverse procedure can be used for removing the parasitic load. Automatic commutation will occur since the waveform reverses polarity every half cycle.

Thus, a control for the parasitic load that uses transistors will involve a greater number of devices than a control that uses SCR's. In addition, this control will add considerable weight to the system because of the transformers. Although control by SCR's will require a small amount of filtering and some additional control circuitry, this approach appears preferable.

Although much work remains to be done before a complete system can be tested, the variable parasitic-load method for speed control appears to be more advantageous than the other schemes mentioned in Chapter I for the following reasons:

1. Since the design of the control involves mainly solid state components, which have no wear-out mode as long as they are operated well within their specifications, the control will probably prove to be the most reliable over a long service life.

2. The design of the control is easily adapted to the design of dynamic power systems presently under study.

3. The control, involving only one simple network in addition to sensing, reference, and parasitic-load subsystems, is the least complex of the schemes mentioned. This simplicity means that the control will probably be the most economical to develop.

CHAPTER VI

CONCLUSIONS

This investigation has shown that the concept of a parasitic-load speed control for dynamic space power systems is valid. An experimental control, which consisted of a compensation network designed according to the mathematical model and an analog simulation of the frequency sensor and parasitic load, responded in the predicted manner to changes in load on an analog-simulated CRU. Although in the actual control some errors will be introduced by the frequency sensor and parasitic load, these errors can be minimized by judicious design of these subsystems and by careful selection of components for these designs. The response of the actual parasitic-load speed control should then be very similar to the response of the experimental control.

For this study a specification for the response of the control was chosen based on expected loads of spacecraft utilizing dynamic power systems. As these requirements become more clearly defined, this specification might change. In this case, the model provides for modification of the compensation network for other responses that are chosen within the following guide lines:

1. Frequency deviations of ±5 per cent.
2. Constant input power to the turbine.

3. Linear relationship between output frequency and output of the frequency sensor.

4. Linear relationship between the output of the compensation network and the amount of parasitic load applied to the alternator.

This study represents only the preliminary work that must be done before a parasitic-load speed control becomes a reality. Much design work, especially in the case of the parasitic load, is needed. After this phase has been completed, the assembled control must be subjected to extensive operational life tests to determine the reliability of the system. Results of these tests should indicate whether or not additional work is necessary before the system can be committed to a flight project.

BIBLIOGRAPHY

BIBLIOGRAPHY

Dauterman, W. E. "Snap 2 Power Conversion System Topical Report No. 18," Thompson Ramo Wooldridge Inc. Report No. ER-5075, 1963.

Lalli, V. R. "Sunflower Rotational Speed Control Topical Report," Thompson Ramo Wooldridge Inc. Report No. ER-4947, 1963.

McKhann, G. G. Preliminary Design of a Pu-238 Isotope Brayton-Cycle Power system for MORL. 4 volumes. Santa Monica, California: Douglas Missile and Space Systems Division, Douglas Aircraft Co., 1965.

"Operational Amplifier Static Gain Errors Analysis and Nomographs," Union Carbide Electronics AN-7, 1966.

Tew, Roy C., and others. "Analog-Computer Study of Parasitic-Load Speed Control for Solar-Brayton System Turboalternator," National Aeronautics and Space Administration TN D-3784, 1967.

Thomas, Ronald L. "Turboalternator Speed Control with Valves in Two-Spool Solar-Brayton System," National Aeronautics and Space Administration TN D-3783, 1967.

Truxal, John G. Automatic Feedback Control System Synthesis. New York: McGraw-Hill Book Company, Inc., 1955.

Weden, C. V. "Operational Amplifier Principles." Orbit, (January, 1955), 9-15.

Word, John L., and others. "Static Parasitic Speed Controller for Brayton-Cycle Turboalternator," National Aeronautics and Space Administration TN D-4776, 1967.

APPENDICES

APPENDIX I

ELECTROMECHANICAL RELATIONSHIPS FOR A SYNCHONOUS ALTERNATOR

Operation of a synchronous alternator can be expressed in terms of three classes of torque acting on the rotating unit: an inertia torque, $T_i(t)$; an electromagnetic torque, $T_e(t)$; and a mechanical shaft torque, $T_{sh}(t)$. Since the mechanical input must supply the electromagnetic and inertia torques, the relationship becomes:

$$T_{sh}(t) = T_i(t) + T_e(t)$$

where all torques are given in units of lb-ft. The inertia torque is given by the product of the moment of inertia of the rotating unit and the angular acceleration. This torque will be:

$$T_i(t) = J \frac{2}{p} \frac{d^2\delta(t)}{dt^2}$$

where δ is an angle in electrical radians between a point on the shaft and a synchronously rotating reference, J is the inertia of the rotating unit in slug-ft^2, and p is the number of poles on the alternator. Since 2/p converts electrical radians to mechanical radians and since angular velocity is the derivative of shaft position, the inertia torque may be written as:

$$T_i(t) = J \frac{d\omega(t)}{dt}$$

whereby

$$T_{sh}(t) = J \frac{d\omega(t)}{dt} + T_e(t) \qquad (21)$$

where $\omega(t)$ is the angular velocity of the rotating members in radians per second.

By converting the angular velocity to revolutions per minute and using the relationship between the number of poles of the alternator, the velocity of the rotating unit and the output frequency, equation (21) will become

$$T_{sh}(t) = \frac{4\pi}{p} J \frac{df(t)}{dt} + T_e(t)$$

By rearranging and integrating, this equation can be solved for the output frequency.

$$\frac{4\pi}{p} J \frac{df(t)}{dt} = T_{sh}(t) - T_e(e)$$

$$\frac{df(t)}{dt} = \frac{p}{4\pi J} \left[T_{sh}(t) - T_e(t)\right]$$

$$f(t) = \frac{p}{4\pi J} \int \left[T_{sh}(t) - T_e(t)\right] dt + C$$

Since the output frequency will equal the design frequency, F_o, for $T_{sh}(t) - T_e(t)$ equal to zero, this equation becomes

$$f(t) = \frac{p}{4\pi J} \int \left[T_{sh}(t) - T_e(t)\right] dt + F_o$$

APPENDIX II

MODIFICATION OF ALTERNATOR TORQUE EQUATIONS

The relationship between the torques acting on the alternator is given in Appendix I as

$$T_i(t) = T_{sh}(t) - T_e(t)$$

This equation can be converted to one involving power by multiplying each side by the angular velocity of the rotating shaft.

$$\omega(t)T_i(t) = \omega(t)T_{sh}(t) - \omega(t)T_e(t)$$

or

$$= P_{sh}(t) - P_e(t)$$

where all power is in watts. The inertia torque was found in Appendix I to be

$$T_i(t) = \frac{4\pi}{p} J \frac{df(t)}{dt}$$

If

$$\omega(t) = \frac{4\pi}{p} f(t)$$

Then

$$\omega(t)T_i(t) = \left(\frac{4\pi}{p} \right)^2 Jf(t) \frac{df(t)}{dt} \qquad (22)$$

where $\omega(t)T_i(t)$ is in units of lb-ft/sec. When the units are converted to watts, equation (22) becomes

$$\frac{21.7\pi^2 J}{p^2} f(t) \frac{df(t)}{dt} = P_{sh}(t) - P_e(t)$$

APPENDIX III

THEORETICAL DETERMINATION OF OUTPUT FREQUENCY

Using the simplest form for the compensation transfer function,

$$G_c(s) = - K_c \frac{s + Z_o}{s}$$

the system transfer function for a disturbance input becomes

$$\frac{F(s)}{P_l(s)} = \frac{- K_i s}{s^2 + 2\zeta\omega_n s + \omega_n^2}$$

where $F(s)$ is the output frequency, $P_l(s)$ is the alternator load, ω_n is the natural frequency of the system, and ζ is the damping ratio. If a load of magnitude K_p is removed from the alternator, the output frequency will be

$$F(s) = \frac{- K_i s(- K_p/s)}{s^2 + 2\zeta\omega_n s + \omega_n^2}$$

$$F(s) = \frac{K_i K_p}{s^2 + 2\zeta\omega_n s + \omega_n^2}$$

By using partial fraction expansion,

$$F(s) = \frac{K_i K_p}{\left[s + \zeta\omega_n - \omega_n(\zeta^2 - 1)^{1/2}\right]\left[s + \zeta\omega_n + \omega_n(\zeta^2 - 1)^{1/2}\right]}$$

$$F(s) = K_i K_p \left[\frac{A}{s + \zeta\omega_n - \omega_n(\zeta^2 - 1)^{1/2}} + \frac{B}{s + \zeta\omega_n + \omega_n(\zeta^2 - 1)^{1/2}}\right] \qquad (23)$$

$$A = \left.\frac{s + \zeta\omega_n - \omega_n(\zeta^2 - 1)^{1/2}}{\left[s + \zeta\omega_n - \omega_n(\zeta^2 - 1)^{1/2}\right]\left[s + \zeta\omega_n + \omega_n(\zeta^2 - 1)^{1/2}\right]}\right|_{s=-\zeta\omega_n+\omega_n(\zeta^2-1)^{1/2}}$$

$$A = \frac{1}{-\zeta\omega_n + \omega_n(\zeta^2 - 1)^{1/2} + \zeta\omega_n + \omega_n(\zeta^2 - 1)^{1/2}}$$

$$A = \frac{1}{2\omega_n(\zeta^2 - 1)^{1/2}} \tag{24}$$

$$B = \left.\frac{s + \zeta\omega_n + \omega_n(\zeta^2 - 1)^{1/2}}{\left[s + \zeta\omega_n - \omega_n(\zeta^2 - 1)^{1/2}\right]\left[s + \zeta\omega_n + \omega_n(\zeta^2 - 1)^{1/2}\right]}\right|_{s=-\zeta\omega_n-\omega_n(\zeta^2-1)^{1/2}}$$

$$B = \frac{1}{-\zeta\omega_n - \omega_n(\zeta^2 - 1)^{1/2} + \zeta\omega_n - \omega_n(\zeta^2 - 1)^{1/2}}$$

$$B = -\frac{1}{2\omega_n^2(\zeta^2 - 1)^{1/2}} \tag{25}$$

Combining equations (23), (24), and (25) gives

$$F(s) = \frac{K_i K_p}{2\omega_n(\zeta^2 - 1)^{1/2}}\left[\frac{1}{s + \zeta\omega_n - \omega_n(\zeta^2 - 1)^{1/2}} - \frac{1}{s + \zeta\omega_n + \omega_n(\zeta^2 - 1)^{1/2}}\right] \tag{26}$$

In the time domain equation (26) is equivalent to

$$f(t) = \frac{K_i K_p}{2\omega_n(\zeta^2 - 1)^{1/2}}\left\{e^{\left[-\zeta\omega_n+\omega_n(\zeta^2-1)^{1/2}\right]t} - e^{\left[-\zeta\omega_n-\omega_n(\zeta^2-1)^{1/2}\right]t}\right\}$$

By rearranging

$$f(t) = \frac{K_i K_p}{2\omega_n(\zeta^2 - 1)^{1/2}} e^{-\zeta\omega_n t}\left[e^{\omega_n(\zeta^2-1)^{1/2}t} - e^{-\omega_n(\zeta^2-1)^{1/2}t}\right]$$

Recognizing that $(e^{x} - e^{-x})/2$ is equivalent to the hyperbolic sine of x, one can rewrite f(t) as

$$f(t) = \frac{K_i K_p}{\omega_n(\zeta^2 - 1)^{1/2}} e^{-\zeta\omega_n t} \sinh\left[\omega_n(\zeta^2 - 1)^{1/2} t\right] \qquad (27)$$

APPENDIX IV

SOLUTION FOR THE MAXIMUM VALUE OF OUTPUT FREQUENCY

The output frequency is given by equation (27).

$$f(t) = \frac{K_i K_p}{\omega_n(\zeta^2 - 1)^{1/2}} e^{-\zeta\omega_n t} \sinh\left[\omega_n(\zeta^2 - 1)^{1/2} t\right] \qquad (27)$$

The maximum value of f(t) can be found by taking the first derivative of this equation and setting the derivative equal to 0.

$$\frac{df(t)}{dt} = K_T \omega_n(\zeta^2 - 1)^{1/2} e^{-\zeta\omega_n t} \cosh\left[\omega_n(\zeta^2 - 1)^{1/2} t\right]$$

$$- K_T \zeta\omega_n e^{-\zeta\omega_n t} \sinh\left[\omega_n(\zeta^2 - 1)^{1/2} t\right]$$

where

$$K_T = \frac{K_i K_p}{\omega_n(\zeta^2 - 1)^{1/2}}$$

$$\frac{df(t)}{dt} = K_T \omega_n e^{-\zeta\omega_n t}\left\{(\zeta^2 - 1)^{1/2} \cosh\left[\omega_n(\zeta^2 - 1)^{1/2} t\right] - \zeta \sinh \omega_n(\zeta^2 - 1)^{1/2} t\right\} \qquad (28)$$

Let

$$\theta = \cosh^{-1}\zeta$$

Then

$$\cosh \theta = \zeta$$

Since

$$\cosh^2 \theta - \sinh^2 \theta = 1 \tag{29}$$

$$\sinh \theta = (\cosh^2 \theta - 1)^{1/2}$$

or

$$\sinh \theta = (\zeta^2 - 1)^{1/2} \tag{30}$$

Substituting equations (29) and (30) into equation (28) gives

$$\frac{df(t)}{dt} = K_T \omega_n e^{-\zeta\omega_n t} \left\{ \sinh \theta \cosh\left[\omega_n(\zeta^2 - 1)^{1/2} t\right] - \cosh \theta \sinh\left[\omega_n(\zeta^2 - 1)^{1/2} t\right] \right\} \tag{31}$$

By using the trigonometric identity for the hyperbolic sine of the difference of two angles, equation (31) becomes

$$\frac{df(t)}{dt} = K_T \omega_n e^{-\zeta\omega_n t} \sinh\left[\theta - \omega_n(\zeta^2 - 1)^{1/2} t\right] \tag{32}$$

To find t_{max} set equation (32) equal to 0.

$$K_T \omega_n e^{-\zeta\omega_n t_m} \sinh\left[\theta - \omega_n(\zeta^2 - 1)^{1/2} t_m\right] = 0$$

For finite t_m, $\omega_n e^{-\zeta\omega_n t_m}$ will not equal 0 and for ζ equal to 1, $K_T \sinh\left[\theta - \omega_n(\zeta^2 - 1)^{1/2} t_m\right]$ may be indeterminant.

Therefore, for $\zeta \neq 1$ and $K_T \neq 0$

$$\sinh\left[\theta - \omega_n(\zeta^2 - 1)^{1/2} t_m\right] = 0$$

or

$$\theta - \omega_n(\zeta^2 - 1)^{1/2}t_m = 0$$

$$\omega_n(\zeta^2 - 1)^{1/2}t_m = \theta$$

$$t_m = \frac{\theta}{\omega_n(\zeta^2 - 1)^{1/2}} \tag{33}$$

The hyperbolic sine can be expanded in a power series and multiplied by K_T to give

$$K_T\sinh\left[\theta - \omega_n(\zeta^2 - 1)^{1/2}t_m\right] = K_T\left\{\theta - \omega_n(\zeta^2 - 1)^{1/2}t_m + \frac{\left[\theta - \omega_n(\zeta^2 - 1)^{1/2}t_m\right]^3}{3!} + \cdots\right\}$$

$$= \frac{K_iK_p}{\omega_n}\left[\frac{\theta}{(\zeta^2 - 1)^{1/2}} - \omega_n t_m + \frac{\theta^3}{3!(\zeta^2 - 1)^{1/2}} - \frac{\omega_n^3(\zeta^2 - 1)t_m^3}{3!} + \cdots\right] \tag{34}$$

Taking the limit of equation (34) as ζ approaches 1 and using $\sinh\theta = (\zeta^2 - 1)^{1/2}$ gives

$$\lim_{\zeta \to 1} K_T\sinh\left[\theta - \omega_n(\zeta^2 - 1)^{1/2}t_m\right] = \frac{K_iK_p}{\omega_n}\left(-\omega_n t_m + \frac{\sinh\theta}{\sinh\theta}\right) \tag{35}$$

If equation (35) is set equal to 0, t_{max} for $\zeta = 1$ can be found.

$$\frac{K_i K_p}{\omega_n}(1 - \omega_n t_m) = 0$$

$$\omega_n t_m = 1$$

$$t_m = \frac{1}{\omega_n} \tag{36}$$

By using the expression $\sinh \theta \; (\zeta^2 - 1)^{1/2}$ in equation (33) and taking the limit as ζ approaches 1

$$\lim_{\zeta \to 1} t_m = \lim_{\zeta \to 1} \frac{\theta}{\omega_n \sinh \theta}$$

and since

$$\lim_{\zeta \to 1} \frac{\theta}{\sinh \theta} = 1$$

$$\lim_{\zeta \to 1} t_m = \frac{1}{\omega_n} \tag{37}$$

Since equations (36) and (37) are identical, equation (33) holds for all ζ's. By using this value for t_m in equation (27), $f_{max}(t)$ can be found.

$$f_{max}(t) = \frac{K_i K_p}{\omega_n(\zeta^2 - 1)^{1/2}} e^{-\zeta \omega_n \left[\frac{\cosh^{-1} \zeta}{\omega_n(\zeta^2 - 1)^{1/2}}\right]} \left[\sinh \omega_n(\zeta^2 - 1)^{1/2} \frac{\cosh^{-1} \zeta}{\omega_n(\zeta^2 - 1)^{1/2}}\right]$$

$$= \frac{K_i K_p}{\omega_n(\zeta^2 - 1)^{1/2}} e^{-\frac{\zeta \cosh^{-1} \zeta}{(\zeta^2 - 1)^{1/2}}} \sinh \cosh^{-1} \zeta$$

$$f_{max}(t) = \frac{K_i K_p}{\omega_n} e^{-\frac{\zeta \cosh^{-1} \zeta}{(\zeta^2 - 1)^{1/2}}}$$

APPENDIX V

ELECTRICAL CHARACTERISTICS OF LM 201

Parameter	Conditions	Maximum	Typical	Minimum	Units
Supply Voltage		±22			V
Power Dissipation		250			mW
Differential Input Voltage		±30			V
Operating Temperature		±150		-65	°C
Input Offset Voltage	T = 25°C $R_S \leq$ 10k	7.5	2.0		mV
Input Offset Current	T = 25°C	500	100		nA
Input Bias Current	T = 25°C	1.5	0.25		µA
Input Resistance	T = 25°C		400	150	kΩ
Output Resistance	T = 25°C	530	200		
Supply Current	T = 25°C V = ±20V	3.0	1.8		mA
Output Voltage	V = ±15V R_L = 10kΩ		±14	±12	V
Swing	R_L = 2kΩ		±13	±10	V
Input Voltage Range	V = 15V			±12	V

ELECTRICAL CHARACTERISTICS OF LM 201.- Concluded.

Parameter	Conditions	Maximum	Typical	Minimum	Units
Common Mode Rejection Ratio	$R_s \leq 10k\Omega$		90	65	db
Supply Voltage Rejection Ratio	$R_s \leq 10k\Omega$		90	70	db
Open Loop Gain	C = 30 pf		105	90	db
Unity Gain Crossover Frequency	C = 30 pf		900	190	kHz

APPENDIX VI

DETERMINATION OF INPUT AND FEEDBACK IMPEDANCES FOR THE COMPENSATION NETWORK

The input and feedback impedances for the amplifier of Figure 6 can be determined by equating the transfer function for this circuit to the transfer function for the compensation desired.

The transfer function for the preamplifier is given by the ratio of the output to input voltages.

$$\frac{V_o}{V_e} = \frac{Z_2}{Z_1} = A$$

The transfer function for the compensation amplifier is given by

$$\frac{V_p}{V_i} = - \frac{Z_f}{Z_i}$$

Since the output of the preamplifier is equal to the input of the compensation amplifier, the combined transfer function is given by

$$\frac{V_p}{AV_e} = - \frac{Z_f}{Z_i}$$

or

$$\frac{V_p}{V_e} = - A \frac{Z_f}{Z_i}$$

This transfer function is equated to $G_c(s)$.

$$- A \frac{Z_f}{Z_i} = - K_c \frac{s + Z_o}{s}$$

By rearranging

$$\frac{Z_f}{Z_i} = \frac{K_c}{A}\,\frac{s + Z_o}{s}$$

$$\frac{Z_f}{Z_i} = \frac{K_c}{A} + \frac{K_c Z_o}{As}$$

Since amplifiers with capacitors in the input are more susceptible to noise than those without, a single resistor will be used as the input impedance. The feedback impedance will then become

$$Z_f = \frac{R_i K_c}{A} + \frac{1}{\frac{A}{R_1 K_c Z_o}\,s}$$

This impedance takes the same form as an R-C series network where the resistance and capacitance are given by

$$R_f = \frac{R_i K_c}{A}$$

$$C_f = \frac{A}{R_i K_c Z_o}$$

The gain of the preamplifier, A, can be represented by the ratio of two resistors.

$$A = \frac{R_2}{R_1}$$

APPENDIX VII

DIGITAL COMPUTER PROGRAM

```
      PROGRAM  AO650   (INPUT,OUTPUT,TAPE5=INPUT,TAPE6=OUTPUT)
      NAMELIST/NAM1/FR,AJ,AKP,P
      READ(5,NAM1)
    9 FORMAT(7E16.8)
    8 FORMAT(1X,5HALPHA,11X,4HZETA,12X,4HTIME,12X,,2HZO,14X,2HKC,14X,2HW
     1N,14X,4HF(T))
      WRITE(6,8)
      AKI=P**2./(68.4*3.14159265*AJ*FR)
      DO1I=1,5
      ALP=FLOAT(I)/100.
      DO2J=1,9
      ZETA=FLOAT(J)/10.
      B=ACOS(ZETA)
      ZO=((AKP*AKI)/(2.*ZETA*ALP*FR))*EXP((-ZETA*B)/((1.-ZETA**2.)**.5))
      AKC= ((2.*ZETA*AKP)/(ALP*FR))*EXP((-ZETA*B)/((1.-ZETA**2.)**.5))
      WN=(AKI*AKC*ZO)**.5
      DO3K=1,151
      KKK=K-1
      TIME=FLOAT(KKK)/50.
      FT=AKP*((AKI/(AKC*ZO*( 1.-ZETA **2.)))**.5)*EXP(-ZETA*WN*TIME)*SIN
     1(WN*((1.-ZETA**2.)**.5)*TIME)
      WRITE(6,9)ALP,ZETA,TIME,ZO,AKC,WN,FT
    3 CONTINUE
    2 CONTINUE
      DO4J=10,10
      ZETA=FLOAT(J)/10.
      ZO=(AKP*AKI*EXP(-1.))/(2.*ALP*FR)
      AKC=(2.*AKP*EXP(-1.))/(ALP*FR)
      WN=.AKP*AKI*EXP(-1.))/(ALP*FR)
      DO5K=1,151
      KKK=K-1
      TIME=FLOAT(KKK)/50.
      FT=AKP*AKI*TIME*EXP(-AKP*AKI*EXP(-1.)*TIME /(ALP*FR))
      WRITE(6,9)ALP,ZETA,TIME,ZO,AKC,WN,FT
    5 CONTINUE
    4 CONTINUE
      DO6J=11,12
      ZETA=FLOAT(J)/10.
      THE=ALOG (ZETA+(ZETA**2.-1.)**.5)
      ZO=((AKP*AKI)/(2.*ZETA*ALP*FR))*EXP((-ZETA*THE)/(((ZETA**2.)-1.)**
     1.5))
      AKC=((2.*ZETA*AKP)/(ALP*FR))*EXP((-ZETA*THE)/(((ZETA**2.)-1.)**.5)
```

```
     1)
      WN=(AKI*AKC*Z0)**.5
      DO7K=1,151
      KKK=K-1
      TIME=FLOAT(KKK)/50.
      V=WN*((ZETA**2.-1.)**.5)*TIME
      FT=AKP*((AKI/(AKC*Z0*(ZETA**2.-1.)))**.5)*EXP(-ZETA*WN*TIME)*(TANH
     1(V)/((1.-TANH(V)**2.)**.5))
      WRITE(6,9)ALP,ZETA,TIME,Z0,AKC,WN,FT
    7 CONTINUE
    6 CONTINUE
    1 CONTINUE
      END
```